Effect of LOS/NLOS Propagation on 5G Ultra-Dense Networks

Galiotto, Carlo; Pratas, Nuno; Doyle, Linda; Marchetti, Nicola

Published in:
Computer Networks

DOI (link to publication from Publisher):
10.1016/j.comnet.2017.04.012

Publication date:
2017

Document Version
Early version, also known as pre-print

Effect of LOS/NLOS Propagation on 5G Ultra-Dense Networks

Carlo Galiotto[1], Nuno K. Pratas[2], Linda Doyle[1], Nicola Marchetti[1]

1) CONNECT, Trinity College Dublin, Ireland

2) Department of Electronic Systems, Aalborg University (AAU), Denmark

1) {galiotc, Linda.Doyle, marchetn}@tcd.ie, 2) nup@es.aau.dk.

Abstract

The combined presence of Line-of-Sight (LOS) and Non-Line-of-Sight (NLOS) components in the radio propagation environment can severely degrade the Ultra-Dense Networks (UDNs) performance. Backed by a stochastic geometry model, we show that when the LOS/NLOS propagation components are taken into account, and as the cell density increases, UDNs suffer from low coverage and the Area Spectral Efficiency (ASE) grows sub-linearly. However, we show that this performance drop can be compensated by increasing the frequency reuse factor or by steering the network into the partial load regime, which occurs when the base stations outnumber the users. In the former, it emerges that frequency reuse improves the ASE vs coverage trade-off of cell densification with respect to a traditional full frequency reuse, provided there is a degree of freedom on the density of cells; in addition, this trade-off improves with the frequency reuse factor N. Finally, we investigate the energy efficiency of UDNs for which we show that, as a combined result of LOS/NLOS propagation and partial load regime, up to two optimal base station densities exist. As a whole, our work provides novel insights on how to overcome the limitations and to take advantage of extreme cell densification in the upcoming 5G wireless networks.

Index Terms

Ultra-dense, LOS/NLOS, Area Spectral Efficiency, partial load, energy efficiency, coverage.

I. Introduction

Ultra-Dense Networks are foreseen as a key enabler for the 5^{-th} generation (5G) wireless networks [1], [2], where a 1000-fold increase in data rates and a 10-fold increase in energy efficiency are expected with respect to current 4G systems [3]. Although a concept rather

than a precise definition, the term *Ultra-Dense Networks* (UDNs) is used to describe networks characterized by a massive and dense deployment of small-cells, in which the density of Base Stations (BSs) may exceed the density of user devices [4]. The degree of deployment density can be used to classify UDNs into two regimes: (i) *full load regime*, i.e., networks in which all the BSs are active; and (ii) *partial load regime*, i.e., networks in which some BSs might be inactive, due to the BSs outnumbering the users.[1]

In [5] it was shown that the Area Spectral Efficiency (ASE) grows linearly with the BS deployment density. This observation was the result of a simplified propagation model. Recent works [6]–[9], which assume realistic propagation models, have shown more conservative ASE gains. Furthermore, when the BS deployment density increases beyond the user density – the network enters the partial load regime – the network will experience a coverage improvement at the expense of reduced ASE gains [4], [10]. This trend implies that a larger density of BSs will be required so to meet the targeted rates, translating on higher network infrastructures costs. In this paper we show that this performance deterioration can be overcome by: (1) steering the network into a partial load regime and (2) leveraging the network frequency reuse.

A. Related Work

In recent years, stochastic geometry has been gradually accepted as a mathematical tool for performance assessment of wireless networks. In fact, the cornerstone of the cell densification studies can be found in [5], where the authors proposed a stochastic geometry-based framework to model single-tier cellular wireless networks. The simplifying assumption of a single slope path loss model, has led the authors to conclude that the ASE has a linear dependence with the cell deployment density. Yet, in subsequent studies, where multi-slope path loss models are assumed [6]–[9], it was shown that the ASE exhibits instead a non-linear behavior with the cell deployment density. This has been observed for both millimeter-wave [6], [11] and sub-6 GHz [8], [9] propagation models. In [6], the authors extended the stochastic geometry framework in [5] to a multi-slope path loss model. The authors in [11] developed a stochastic geometry framework for path-loss including Line-of-Sight (LOS) and Non-Line-of-Sight (NLOS). The effect of NLOS propagation on the outage probability has been studied in [7], where the authors

[1]This can be the result of a reduced load in terms of users or of a massive deployment of BSs.

propose a function that gives the LOS probability at a given point depending on the distance from the source, the average size of the buildings and their deployment density. In our previous work [8] and in [9], the performance of the network with a combined LOS/NLOS has been modeled and evaluated.

All these studies assume that all base stations are active and have at least one user to serve, which is not always the case in a ultra-dense network setting. In fact, some recent studies indicate [4], [12] that the Base Station (BS) deployment density, in 5G wireless networks, is expected to increase even beyond that of the users; implying that some BSs will have no users to serve and will therefore remain inactive. Motivated by this, we broaden in this paper the body of work on UDNs towards networks on a *partial load regime*.

Previous work on stochastic geometry for partially loaded networks has appeared in [4], [10], [13], [14]. The authors in [13] studied the coverage in single-tier networks, while multi-tier networks are addressed in [14]. An analysis of the ASE of partially loaded networks has been carried out in [4], while in [10] the authors have extended the stochastic geometry-based model further to include multi-antenna transmission, and have also assessed the energy efficiency. Overall, the authors in [10], [13], [14] have shown that the network coverage improves as the BS deployment density increases beyond the user density; however, the ASE gain turns out to be reduced and grows logarithmically with the BS deployment density. Nonetheless, the authors in [10], [13], [14] modeled the propagation according to a single slope path-loss model and did not investigate the effect of LOS/NLOS propagation when the network is in a partial load regime.

We reckon that the study of UDNs should not ignore the joint effects that both LOS/NLOS propagation and partial load regime have on the network performance. This paper is to our knowledge the first contribution that combines these two effects and provides a complete analysis of its effect on the behavior of the ASE, coverage, and energy efficiency in a UDN setting.

B. Our Contribution

In this paper we investigate the cell densification process in UDNs and evaluate the effect of LOS/NLOS propagation on the coverage, spectral efficiency, ASE, and energy efficiency. Overall, the major contributions of our work can be summarized in the following points:

1) Stochastic geometry-based model for UDNs with LOS/NLOS propagation: The model we propose allows us to study the Signal-to-Interference-plus-Noise-Ratio (SINR) distribution,

the spectral efficiency and the ASE of UDNs with the LOS/NLOS propagation components. Our model is suited to investigate the performance trend of network densification in 5G-like scenarios, while modeling UDNs in both full and partial load regimes[2].

2) Investigation on the combined effect of LOS/NLOS propagation, partial load regime and frequency reuse on UDNs performance: We show that the LOS/NLOS propagation affects the UDNs' key performance metrics negatively. Specifically, the ASE exhibits sub-linear gain and a drastic coverage drop as the deployment density goes beyond 300 BSs/km^2. This performance deterioration can be circumvented by leveraging frequency reuse and steering the UDN towards a partial load regime. For instance, increasing the BS density beyond that of the users increases the network coverage and negates the impact of LOS/NLOS propagation. Further, frequency reuse achieves better ASE vs. coverage trade-offs as the frequency reuse factor increases, compared to a reuse factor 1. Hence, we provide design guidelines on how to overcome the inherent limitations and take advantage of extreme cell densification.

3) Investigation on the effect of LOS/NLOS path-loss on UDNs energy efficiency: We show that, as a consequence of the LOS/NLOS propagation, the energy efficiency has a maximum value that occurs at a given base station density; beyond that density, the energy efficiency drops considerably with respect to the case of single slope path-loss, making cell-densification costly from an energetic stand-point. Further, we show that, in a partial load regime, a second local maximum of the energy efficiency can be achieved, provided that the inactive base stations are put into standby mode to save energy. In conclusion, our analysis provides insights on how to optimize the BS deployment density so to achieve optimal energy efficiency.

C. Paper Structure

The remainder of this paper is organized as follows. In Section II we describe the system model. We show our formulation for computing the SINR, SE and ASE in Section III and we address the energy efficiency in Section IV. In Section V we present and discuss the results while the conclusions are drawn in Section VI.

II. System model

We assume a network of small-cell base stations deployed according to a homogeneous and isotropic Spatial Poisson Point Process (SPPP), denoted as $\Phi \subset \mathbb{R}^2$, with intensity λ. Each BS

[2]The partial load regime has been identified as one of the typical scenarios in 5G wireless networks [4], [12].

transmits with an isotropic antenna and power, P_{TX}; we focus our analysis on the downlink.

Let us note that, by definition of the SPPP, each point is independent of any other point of the process and, as a result, base stations may turn out to be located either too close to or too far from one another. This might not be in line with real deployments of cellular networks, where base station locations tend to be planned in such a way to be equidistant from one another, so as to provide uniform coverage. Despite this drawback, SPPPs have been shown to model the network performance metrics with a good level of accuracy; more precisely, they provide a more conservative prediction of the real network performance compared to the less tractable standard hexagonal cell grid, which instead gives an overestimate of it [5]. Thanks to its good trade-off between the mathematical tractability and accuracy, we model the small-cell base station network as an SPPP.

A. Channel model

In our analysis, we consider the following path loss model:

$$\mathrm{PL}(d) = \begin{cases} K_{\mathrm{L}} d^{-\beta_{\mathrm{L}}} & \text{with probability } p_{\mathrm{L}}(d), \\ K_{\mathrm{NL}} d^{-\beta_{\mathrm{NL}}} & \text{with probability } 1 - p_{\mathrm{L}}(d), \end{cases} \tag{1}$$

where β_{L} and β_{NL} are the path-loss exponents for LOS and NLOS propagation, respectively; K_{L} and K_{NL} are the signal attenuations at distance $d = 1$ m for LOS and NLOS propagation, respectively; $p_{\mathrm{L}}(d)$ is the probability of having LOS as a function of the distance d. The model given in (1) is recommended in 3GPP to model the LOS/NLOS propagation, for example, in scenarios with Heterogeneous Networks [15, Table A.2.1.1.2-3]. The incorporation of the NLOS component in the path loss model accounts for possible obstructions of the signal due to large scale objects (e.g. buildings), which will result in a higher attenuation of the NLOS propagation compared to the LOS path. A visualization of the LOS and NLOS propagation as a result of the obstruction from buildings is given in Fig. 1.

We further assume that the propagation is affected by Rayleigh fading, which is exponentially distributed $\sim \exp(\mu)$. Although Ricean or Nakagami-m models would more accurately describe the small-scale fading effect of the LOS propagation, Rayleigh model has the advantage of being more tractable than the former ones from a mathematical point of view. In addition to it, Rayleigh fading provides a conservative prediction of the system performance, as it gives a lower bound of the SINR for system models with Nakagami-m fading [16].

TABLE I

LIST OF NOTATIONS

Symbol	Meaning
Φ, Φ_{L}, Φ_{NL}	SPPP of base stations, of base stations in LOS with the user and of base stations in LOS with the user, respectively
$\lambda, \lambda_{\mathrm{L}}(x), \lambda_{\mathrm{NL}}(x)$	Density of BSs, of BSs in LOS with the user and of the BSs in LOS with the user, respectively
λ_{A}, λ_{I}, λ_{U}	Density of active BSs, of the interfering BSs, and of the users, respectively
p_{L}, p_{NL}	LOS and NLOS probability functions, respectively
K_{L}, K_{NL}, K_{eq}	Signal attenuation at distance 1 for LOS propagation, for NLOS propagation and for equivalent model, respectively
β_{L}, β_{NL}, β_{eq}	Path-loss coefficients, for LOS propagation, for NLOS propagation and for equivalent model, respectively
L	LOS likelihood paramter
$f_{\mathrm{eq}}(x)$, $d_{\mathrm{eq}}(d)$	Equivalent point and equivalent distance, respectively, for the NLOS-to-LOS mapping
$f_{\mathrm{eq}}^{-1}(x)$, $d_{\mathrm{eq}}^{-1}(d)$	NLOS point and reversed distance, respectively, for the equivalent-to-NLOS mapping
α, β	Asymptotical slope of ASE and of the transmit power, respectively, as functions of the cell density
P_{TX}, P_{T}	Transmit power per base station (as a function of the cell density) and component (of the transmit power per base station) independent of the cell density, respectively
P_{TOT}, P_0, P_{RF}	Total Transmit power of the network, fixed component of the BS power consumption and power consumption per BS due to emitted RF signal, respectively
K_{RF}	Power loss of the power amplifier
ρ	Power saving factor of a base station in stand-by mode
γ, γ_{th}	SINR and SINR threshold defining the network coverage, respectively
p_{A}	Probability of a base station being active
η_{A}, η_{EE}	Area Spectral Efficiency (ASE) and Energy Efficiency, respectively
E[C]	Average cell spectral efficiency or average typical user rate
BW_{A}, BW_{U}, N	Available bandwidth, used bandwidth and frequency factor reuse, respectively

Regarding the shadow fading, it has been shown that in networks with a deterministic, either regular or irregular, base station distribution affected by log-normal shadow fading, the statistic of the propagation coefficients converges to that of a network with SPPP distribution as the shadowing variance increases [17]. In other words, this SPPP intrinsically models the effect of shadow fading.

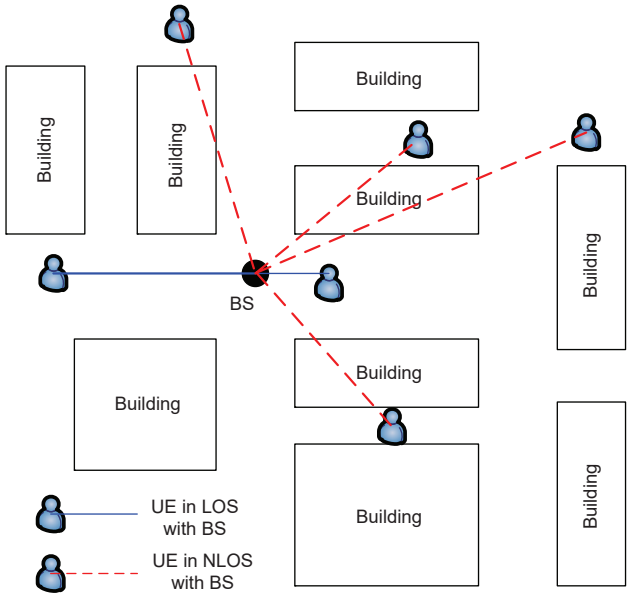

Fig. 1. Representation of the LOS and NLOS propagation in a urban scenario. LOS propagation occurs where there is clear sight between the base station and the user, while NLOS occurs where some large scale objects like buildings are obstructing the path between the transmitter and the receiver.

B. LOS probability function

To ensure that our formulation and the outcomes of our study are general and not limited to a specific LOS probability pattern, we consider two different LOS probability functions. The first one — which we refer to as *LOS Case 1* — is proposed by the 3GPP [15, Table A.2.1.1.2-3] to assess the network performance in pico-cell scenarios; we provide its expression below:

$$p_{\mathrm{L,3G}}(d) = 0.5 - \min\left(0.5, 5\exp\left[-\frac{d_0}{d}\right]\right) + \min\left(0.5, 5\exp\left[-\frac{d}{d_1}\right]\right), \tag{2}$$

where d_0 and d_1 are two parameters that allow (2) to match the measurement data. Unfortunately, this function is not practical for an analytical formulation. Therefore, we chose to approximate it with a more tractable one, namely:

$$p_{\mathrm{L}}(d) = \exp\left(-(d/L)^2\right), \tag{3}$$

where L is a parameter that allows (3) to be tuned to match (2), as discussed in Section V (see Table II). The second function — which we referred to as *LOS Case 2* — is also suggested by the 3GPP [15, Table A.2.1.1.2-3] and is given below:

$$p_{\mathrm{L}}(d) = \exp(-d/L). \tag{4}$$

From a physical stand point, the parameter L can be interpreted as the LOS likelihood of a given propagation environment as a function of the distance.

C. User distribution, fully and partially loaded networks

In our model, we assume that: (i) the users are uniformly distributed according to a homogeneous SPPP of intensity λ_{U} and (ii) each user connects only to one base station, the one from which the path-loss is the minimum. Whenever we consider a finite area A, N_{U} indicates the average number of users in the network. We also assume the users are served with full buffer, i.e., the base station has always data to transmit to the users and makes full use of the available resources.

Depending on the ratio between the density of users and the density of basestations, we distinguish two cases, namely, *full load* and *partial load regime*. By full load we refer to the case where each BS has at least one user to serve. With reference to a real scenario, networks in full load model the case where there are many more users than base stations, so that each base station serves a non-empty set of users. However, when the density of users is comparable or less than of the base stations; some base stations may not have any users to serve and will become inactive (not transmitting nor generating interference). When this occurs, we say that the network is in a partial load regime. The modeling of the network in this regime allows the study of those scenarios characterized by high density of base stations and, in particular, scenarios where the density of base stations exceeds the density of users, such as in UDNs.

To define formally the concepts of full and partial load regime, we start by introducing:

Definition 1 (Probability of a base station being active)**.** *The probability of a base station being active, denoted as p_{A}, is the probability that a base station has at least one user to serve. This event implies that the base station is active and transmits to its users.*

Definition 2 (Full load regime)**.** *The network is said to be in full load regime if each base station has at least one user to serve; this is equivalent to $p_A = 1$.*

Definition 3 (Partial load regime)**.** *The network is said to be in partial load regime if $p_A < 1$.*

Remark 1. To ensure $p_A = 1$, the density of users λ_{U} should tend to infinity. But, as we will discuss in Section III-E2, it is reasonable to assume $p_A = 1$ when $\lambda_{\mathrm{U}} \gg \lambda$.

III. SINR, SPECTRAL EFFICIENCY AND ASE

In this section we develop the analytical model used to compute the SINR Complementary Cumulative Distribution Function (CCDF), which will allow us to assess key performance metrics such as coverage, spectral efficiency and ASE.

A. Procedure to compute the SINR CCDF

We compute the SINR tail distribution (i.e., the Complementary CDF), by extending the analytical framework first proposed in [5] to include the LOS and NLOS components. From the Slivnyak's Theorem [18, Theorem 8.10], we consider the *typical user* as the focus of our analysis, which for convenience is assumed to be located at the origin. The procedure is composed of two steps: (i) we compute the SINR CCDF for the typical user conditioned on the distance from the user to the serving base station, denoted as r; (ii) using the PDF of the distance from the closest BS $f_r(R)$, which corresponds to the serving BS, we can average the SINR CCDF over all possible values of distance r.

Let us denote the SINR by γ; formally, the CCDF of γ is computed as:

$$\mathbb{P}\left[\gamma > y\right] = \mathrm{E_r}\left[\mathbb{P}\left[\gamma > y | r\right]\right] = \int_0^{+\infty} \mathbb{P}\left[\gamma > y | r = R\right] f_r(R) \mathrm{d}R. \tag{5}$$

The key elements of this procedure are the PDF of the distance to the nearest base station $f_r(R)$ and the tail probability of the SINR conditioned on r, $\mathbb{P}\left[\gamma > y | r = R\right]$. The methodology to compute each of these elements and model the LOS/NLOS components will be exposed next.

B. SPPPs of base stations in LOS and in NLOS with the user

The set of the base stations locations originates an SPPP, which we denote by $\Phi = \{x_n\}$.[3] As a result of the propagation model we have adopted in our analysis (see Section II-A), the user can either be in LOS or NLOS with any base station x_n of Φ. Now, we perform the following mapping: we first define the set of LOS points, namely Φ_{L}, and the set of NLOS points, Φ_{NL}. Then, each point x_n of Φ is mapped into Φ_{L} if the base station at location x_n is in LOS with the user, while it is mapped to Φ_{NL} if the base station at location x_n is in NLOS with the user. Since the probability that x_n is in LOS with the user is $p_{\mathrm{L}}(\|x\|)$, it follows that each point x_n of Φ is mapped with probability $p_{\mathrm{L}}(\|x\|)$ into Φ_{L} and probability $p_{\mathrm{NL}}(\|x\|) = 1 - p_{\mathrm{L}}(\|x\|)$ into

[3]Whenever there is no chance of confusion, we drop the subscript n and use x and instead of x_n for convenience of notation.

Φ_{NL}. Given that this mapping is performed independently for each point in Φ, then from the "Thinning Theorem" [18, Theorem 2.36] it follows that the processes Φ_{L} and Φ_{NL} are SPPPs with density $\lambda_{\mathrm{L}}(x) = \lambda p_{\mathrm{L}}(\|x\|)$ and $\lambda_{\mathrm{NL}}(x) = \lambda\left(1 - p_{\mathrm{L}}(\|x\|)\right)$, respectively. Note that, because of the dependence of $\lambda_{\mathrm{L}}(x)$ and $\lambda_{\mathrm{NL}}(x)$ on x, Φ_{L} and Φ_{NL} are inhomogeneous SPPPs. Further, we make the assumption that Φ_{L} and Φ_{NL} are independent processes; the reasons of this choice are given in the following. First, each point of Φ_{L} is independent of each point of Φ_{NL}, because Φ_{L} and Φ_{NL} are the result of an independent sampling from the process Φ, in which each point is independent of one another. Second, the union of two independent SPPPs processes is an SPPP of which the density is the sum of the densities of the individual SPPPs [19, Preposition 1.3.3], the union of Φ_{L} and Φ_{NL} is an SPPP of density $\lambda_{\mathrm{L}}(x) + \lambda_{\mathrm{NL}}(x) = \lambda$, i.e., it is an SPPP with the same density as that of the original process Φ. The validity of the assumption of independence between Φ_{L} and Φ_{NL} is also supported by the close matching with simulation results, as shown in our previous work [8].

C. Mapping the NLOS SPPP into an equivalent LOS SPPP

Given that we have two inhomogeneous SPPP processes, it is not trivial to obtain the distribution of the minimum distance of the user to the serving base station, which will be necessary later on to compute the SINR CDF. In fact, assuming the user to be in LOS with the serving base station at a distance d_1, there might be an interfering BS at a distance $d_2 < d_1$ which is in NLOS with the user. This is possible because the NLOS propagation is affected by a higher attenuation than the LOS propagation.

Hence, to make our problem more tractable, we map the set of points of the process Φ_{NL}, which corresponds to the NLOS base stations, into an equivalent LOS process Φ_{eq}; each point $x \in \Phi_{\mathrm{NL}}$ located at distance d_{NL} from the user is mapped to a point x_{eq} located at distance d_{eq} from the user, so that the BS located at x_{eq} provides the same signal power to the user with path-loss $K_{\mathrm{L}} d_{\mathrm{eq}}^{-\beta_{\mathrm{L}}}$ as if the base station were located at x with path-loss $K_{\mathrm{NL}} d_{\mathrm{NL}}^{-\beta_{\mathrm{NL}}}$.

Definition 4 (Mapping function f_{eq})**.** *We define the mapping function* $f_{\mathrm{eq}} : \Phi_{\mathrm{NL}} \to \Phi_{\mathrm{eq}}$ *as:*

$$f_{\mathrm{eq}}(x) = \frac{x}{\|x\|} d_{\mathrm{eq}}\left(\|x\|\right), \tag{6}$$

$$d_{\mathrm{eq}}(d) = \left(\frac{K_{\mathrm{L}}}{K_{\mathrm{NL}}}\right)^{1/\beta_{\mathrm{L}}} d^{\beta_{\mathrm{NL}}/\beta_{\mathrm{L}}}. \tag{7}$$

Definition 5 (Inverse mapping function $g_{\rm eq}$)**.** *The inverse function* $g_{\rm eq} = f_{\rm eq}^{-1} : \Phi_{\rm eq} \to \Phi_{\rm NL}$ *is defined as:*

$$g_{\rm eq}(x) = \frac{x}{\|x\|} d_{\rm eq}^{-1}\left(\|x\|\right), \tag{8}$$

$$d_{\rm eq}^{-1}(d) = \left(\frac{K_{\rm NL}}{K_{\rm L}}\right)^{1/\beta_{\rm NL}} d^{\beta_{\rm L}/\beta_{\rm NL}} = K_{\rm eq} d^{\beta_{\rm eq}}, \tag{9}$$

where $K_{\rm eq} = \left(\frac{K_{\rm NL}}{K_{\rm L}}\right)^{1/\beta_{\rm NL}}$ *while* $\beta_{\rm eq} = \beta_{\rm L}/\beta_{\rm NL}$.

Note that from the "Mapping Theorem" [18, Theorem 2.34], $\Phi_{\rm eq}$ is still an SPPP.

D. PDF of the distance from the user to the serving BS

Using the mapping we introduced in Section III-C, we can compute the PDF $f_r(R)$ of the minimum distance r between the user and the serving BS. To this end, we first compute the probability $\mathbb{P}\left[r > R\right]$, which is the probability that the serving base station is located at a distance larger than R from the user; the PDF can be ultimately obtained from the derivative of $\mathbb{P}\left[r > R\right]$ as $f_r(R) = \frac{\rm d}{{\rm d}R}(1 - \mathbb{P}\left[r > R\right])$. $\mathbb{P}\left[r > R\right]$ can be computed as the probability that no BS is included within the radius R —i.e., no point of the LOS process $\Phi_{\rm L}$ and no LOS equivalent point of the NLOS process $\Phi_{\rm L}$. In mathematical terms, let $B(0,l)$ be the ball of radius l centred at the origin $(0,0)$. Moreover, we use the notation $\Phi(\mathcal{A})$ to refer to the number of points $x \in \Phi$ contained in $\mathcal{A}$ [18]. Using the mapping we introduced in Section III-C the probability $\mathbb{P}\left[r > R\right]$ can be found as:

$$\begin{aligned}
\mathbb{P}\left[r > R\right] &= \mathbb{P}\left[\Phi_{\rm L}\left(B(0,R)\right) = 0 \cap \Phi_{\rm eq}\left(B\left(0,R\right)\right) = 0\right] \\
&\overset{(a)}{=} \mathbb{P}\left[\Phi_{\rm L}\left(B(0,R)\right) = 0 \cap \Phi_{\rm NL}\left(B\left(0, d_{\rm eq}^{-1}(R)\right)\right) = 0\right] \\
&\overset{(b)}{=} \mathbb{P}\left[\Phi_{\rm L}\left(B(0,R)\right) = 0\right] \cdot \mathbb{P}\left[\Phi_{\rm NL}\left(B\left(0, d_{\rm eq}^{-1}(R)\right)\right) = 0\right],
\end{aligned} \tag{10}$$

where equality (a) comes from the mapping defined in (8) and in (9), while equality (b) comes from the independence of the processes $\Phi_{\rm L}$ and $\Phi_{\rm NL}$. By making use of the independence and by applying the probability function of inhomogeneous SPPP [18, Definition 2.10][4] to each of the factors in (10), we obtain the following,

$$\mathbb{P}\left[r > R\right] = \exp\left(-\int_{B(0,R)} \lambda_{\rm L}(x){\rm d}x\right) \exp\left(-\int_{B\left(0,d_{\rm eq}^{-1}(R)\right)} \lambda_{\rm NL}(x){\rm d}x\right). \tag{11}$$

[4]Given an inhomogeneous SPPP Φ of density $\lambda(x)$, the probability of having no points within a compact set B is $\mathbb{P}\left[\Phi\left(B\right) = 0\right] = \exp\left(-\int_B \lambda(x){\rm d}x\right)$

From (11), we can obtain $f_r(R)$, first, by integrating and, second, by computing its first derivative in R. The formulation in (11) is general and thus can be applied to several LOS probability functions $p_{\mathrm{L}}(d)$. Below, we provide the expression of the PDF of the distance from the UE to the serving BS for the LOS functions (3) and (4), respectively.

Result 1. *If the LOS probability function is as in* (3) *and if we denote* $d_{\mathrm{eq}}^{-1}(R)$ *by* R_{eq}*, the PDF of the distance to the serving BS is:*

$$f_r(R) = -\left(e^{\pi\lambda L^2 e^{-\frac{R^2}{L^2}}} \cdot e^{-\pi\lambda L^2 e^{-\frac{R_{\mathrm{eq}}^2}{L^2}}} \cdot e^{-\pi\lambda R_{\mathrm{eq}}^2} \right) \tag{12}$$

$$\left(-2\pi\lambda R e^{-\frac{R^2}{L^2}} \pi\lambda K_{\mathrm{eq}}^2 2\beta_{\mathrm{eq}} R^{2\beta_{\mathrm{eq}}-1} e^{-\frac{-K_{\mathrm{eq}}^2 R^{2\beta_{\mathrm{eq}}}}{L^2}} - \pi\lambda K_{\mathrm{eq}}^2 2\beta_{\mathrm{eq}} R^{2\beta_{\mathrm{eq}}-1} \right).$$

Result 2. *If the LOS probability function is as in* (4) *and if we denote* $d_{\mathrm{eq}}^{-1}(R)$ *by* R_{eq}*, the PDF of the distance to the serving BS is:*

$$f_r(R) = -\left(e^{2\pi\lambda L^2 e^{-\frac{R}{L}}} \cdot e^{2\pi\lambda L R e^{-\frac{R}{L}}} \cdot e^{-\pi\lambda R_{\mathrm{eq}}^2} \cdot e^{-2\pi\lambda L^2 e^{-\frac{R_{\mathrm{eq}}}{L}}} \cdot e^{-2\pi\lambda L R_{\mathrm{eq}} e^{-\frac{R_{\mathrm{eq}}}{L}}} \right) \tag{13}$$

$$\left(-2\pi\lambda L e^{-\frac{R}{L}} - 2\pi\lambda(L-R) e^{-\frac{R}{L}} - \pi\lambda K_{\mathrm{eq}}^2 2\beta_{\mathrm{eq}} R^{2\beta_{\mathrm{eq}}-1} \right.$$

$$\left. +2\pi\lambda L K_{\mathrm{eq}} \beta_{\mathrm{eq}} R^{\beta_{\mathrm{eq}}} e^{-\frac{K_{eq} R^{\beta_{\mathrm{eq}}}}{L}} + 2\pi\lambda L K_{\mathrm{eq}} \beta_{\mathrm{eq}} R^{\beta_{\mathrm{eq}}-1} (K_{\mathrm{eq}} R^{\beta_{\mathrm{eq}}} - L) e^{-\frac{K_{eq} R^{\beta_{\mathrm{eq}}}}{L}} \right).$$

We refer to the Appendix for the details of the $f_r(R)$ we have given in (12) and in (13).

E. Spatial process of the interfering base stations and of the active base stations

The model we propose in this paper can be extended to the cases of partial load regime and of frequency reuse, which herein we treat separately. In order to do so, we first need to identify the *process of active base stations* and the *process of the base stations interfering with the typical user*, which will be required to obtain the coverage and the area spectral efficiency. We define the active base stations as those BSs having one or more users to serve. A BS which is not active does not transmit and, therefore, does not generate any interference. On the other hand, an active BS can potentially, but not necessarily, be seen as an interferer by the typical user; in particular, an active BS (excluding the one serving the user) acts as an interferer if that BS transmits over the same band used to serve that user. In the following, we denote by Φ_{A} the set of active BSs, while we denote by Φ_{I} the set of the interfering BSs.

1) Frequency reuse: In this case we assume that all the BSs are active, but where each of these only uses a portion of the spectrum, in order to reduce interference in the network. Since all the BSs are active, the process Φ_{A} is the same as Φ. Further, we assume that each BS selects a channel randomly [20]; using a frequency reuse factor of N, each BS uses 1 out of N channels, chosen independently of the other BSs. Hence, each BS interferes with a given user with probability $1/N$; this is equivalent to carrying out a thinning of the original process Φ with probability $1/N$; from the Thinning Theorem [18, Theorem 2.36], we obtain that Φ_{I} is a homogeneous process with density $\lambda_{\mathrm{I}} = \lambda/N$.

2) Partial and full load regime: In the partial load regime, we recall from Section II-C that a fraction of the base stations might be inactive and will not generate interference. Assuming all the BSs transmit over the same band, then only the BSs active will generate interference to the users – with the exception of the serving BS. Thus, we can write $\Phi_{\mathrm{I}} = \Phi_{\mathrm{A}} \setminus x_0$, where x_0 is the serving base station; moreover, from the Palm Theorem [18], Φ_{I} and Φ_{A} have the same density. To obtain the process of active BSs Φ_{A} from the original process Φ, we first assume that each user deployed in the network connects to the BS with the minimum path-loss; finally, only the BSs which are assigned one or more users will be picked to form the set Φ_{A}. However, the fact that a BS is picked to be part of Φ_{A} depends on the positions of the neighboring BSs, which implies that the BSs belonging to Φ_{A} are not picked independently of one another [13].

As the independence among the points of a process is a necessary condition in order to have an SPPP, it follows that Φ_{A} cannot be formally regarded as such; to circumvent this issue and make Φ_{A} more mathematically tractable, in some previous work [10], [13] the authors proposed to approximate Φ_{A} with an SPPP. Specifically, the authors in [13] have shown that; (i) the probability p_{A} of a base station to be active (i.e., to have users to serve) can be well approximated once the density of users λ_{U} and density of base stations λ are know; and (ii) the process Φ_{A} of active base stations can be well approximated by an SPPP, obtained through the thinning the original process Φ with probability p_{A}, which is given below [13]:

$$p_{\mathrm{A}} = 1 - \left(1 + \frac{\lambda_{\mathrm{U}}}{3.5\lambda}\right)^{-3.5}. \tag{14}$$

Although (14) has been proved to be a valid approximation for single slope path-loss models—for which the user association to the BS is based on the minimum distance—we extend the

use of this approximation to the LOS/NLOS path-loss model given in (1).[5] Hence we model the process of active BSs as an SPPP, which, based on the Thinning Theorem, has density $\lambda_{\mathrm{A}} = p_{\mathrm{A}}\lambda$; moreover, as mentioned in Section III-E2, Φ_{A} and Φ_{I} have the same density, i.e., $\lambda_{\mathrm{I}} = \lambda_{\mathrm{A}}$. Fig. 2 shows how the probability p_{A} and the λ_{I} vary as functions of the ratio $\lambda/\lambda_{\mathrm{U}}$.

Remark 2. Based on Fig. 2, we consider fully loaded networks as a special case of partially loaded networks when the density of users λ_{U} is greater than 10λ, for which the approximation $p_{\mathrm{A}} = 1$ holds. For fully loaded network, the processes of the active base stations and of interfering base stations have densities $\lambda_{\mathrm{A}} = \lambda$ and $\lambda_{\mathrm{I}} = \lambda$, respectively.

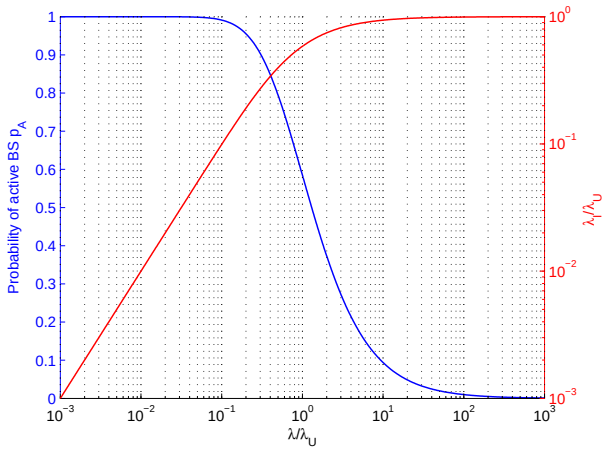

Fig. 2. Probability of a BS being active P_A and density of interfering BS λ_I vs BS density for partially loaded networks. The probability p_{A} drops as the ratio $\lambda/\lambda_{\mathrm{U}}$ is close to or greater than 1, i.e., as λ approaches λ_{U}. As a result of this, the density of active BSs as well as the density of interfering BSs converge to λ_{U} as λ approaches or overcomes λ_{U}.

F. SINR complementary cumulative distribution function

The probability $\mathbb{P}\left[\gamma > y | r = R\right]$ can be computed as in [5, Theorem 1]; we skip the details and provide the general formulation:

$$\mathbb{P}\left[\gamma > y | r = R\right] = \mathbb{P}\left[\frac{gK_{\mathrm{L}}R^{-\beta_{\mathrm{L}}}}{\sigma^2 + I_R} > y\right] = e^{-\mu y K_{\mathrm{L}}^{-1} R^{\beta_{\mathrm{L}}} \sigma^2} \mathcal{L}_{I_R}(\mu y K_{\mathrm{L}}^{-1} R^{\beta_{\mathrm{L}}}), \tag{15}$$

where g is the Rayleigh fading, which we assume to be an exponential random variable $\sim exp(\mu)$; σ^2 is the variance of the additive white Gaussian noise normalized with the respect to the transmit

[5]We refer the reader to Appendix B for the numerical validation of (14) in a LOS/NLOS path-loss model.

power; I_R is the interference conditioned on distance R of the user to the serving BS and can be computed as the sum of the interference from the BSs in LOS with the user and of the interference from the BSs in NLOS with the user, i.e.,

$$I_R = \sum_{\{i:\, x_i \in \Phi_{\mathrm{L}} \cap \Phi_{\mathrm{A}},\, \|x_i\| > R\}} g_i K_{\mathrm{L}} \|x_i\|^{-\beta_{\mathrm{L}}} + \sum_{\{j:\, f_{\mathrm{eq}}(x_j) \in \Phi_{\mathrm{NL}} \cap \Phi_{\mathrm{A}},\, \|f_{\mathrm{eq}}(x_j)\| > R\}} g_j K_{\mathrm{L}} \|x_j\|^{-\beta_{\mathrm{L}}}, \tag{16}$$

where g_i and g_j are independent and identically distributed $\sim exp(\mu)$ fading coefficients. To ensure that the serving BS is excluded from the interferers in (16), I_R accounts only for the LOS BSs (i.e., $\{i : x_i \in \Phi_{\mathrm{L}} \cap \Phi_{\mathrm{A}},\, \|x_i\| > R\}$) and for the LOS-equivalent points (i.e., $\{j : f_{\mathrm{eq}}(x_j) \in \Phi_{\mathrm{NL}} \cap \Phi_{\mathrm{A}},\, \|f_{\mathrm{eq}}(x_j)\| > R\}$) whose distance from the user is greater than R; note that only the active base stations are included among the interferers. By applying the inverse mapping introduced in Definition 5 to the second term of the sum in (16), we obtain:

$$I_R = \sum_{\{i:\, x_i \in \Phi_{\mathrm{L}} \cap \Phi_{\mathrm{A}},\, \|x_i\| > R\}} g_i K_{\mathrm{L}} \|x_i\|^{-\beta_{\mathrm{L}}} + \sum_{\{j:\, x_j \in \Phi_{\mathrm{NL}} \cap \Phi_{\mathrm{A}},\, \|x_j\| > d_{\mathrm{eq}}^{-1}(R)\}} g_j K_{\mathrm{NL}} \|x_j\|^{-\beta_{\mathrm{NL}}} \tag{17}$$

The Laplace transform $\mathcal{L}_{I_R}(s)$ if the interference I_R can be written as follows:

$$\begin{aligned}
\mathcal{L}_{I_R}(s) &= \mathbb{E}_{I_R}[\exp(-sI_R)] \\
&= \mathbb{E}_{\Phi_{\mathrm{L}} \cap \Phi_{\mathrm{A}}, \Phi_{\mathrm{NL}} \cap \Phi_{\mathrm{A}}, g_i, g_j} \Bigg[\exp\Bigg(-s \sum_{\{i:\, x_i \in \Phi_{\mathrm{L}} \cap \Phi_{\mathrm{A}},\, \|x_i\| > \|x_0|\}} g_i K_{\mathrm{L}} \|x_i\|^{-\beta_{\mathrm{L}}} \Bigg) \\
&\exp\Bigg(-s \sum_{\{j:\, x_j \in \Phi_{\mathrm{NL}} \cap \Phi_{\mathrm{A}},\, \|x_j\| > d_{\mathrm{eq}}^{-1}(R)\}} g_j K_{\mathrm{NL}} \|x_j\|^{-\beta_{\mathrm{NL}}} \Bigg) \Bigg].
\end{aligned}$$

Given that Φ_{L} and Φ_{NL} are two independent SPPP, we can separate the expectation to obtain:

$$\begin{aligned}
\mathcal{L}_{I_R}(s) = \mathbb{E}_{\Phi_{\mathrm{L}} \cap \Phi_{\mathrm{A}}, g_i} \Bigg[\exp\Bigg(-s \sum_{\{i:\, x_i \in \Phi_{\mathrm{L}} \cap \Phi_{\mathrm{A}},\, \|x_i\| > R\}} g_i K_{\mathrm{L}} \|x_i\|^{-\beta_{\mathrm{L}}} \Bigg) \Bigg] \\
\mathbb{E}_{\Phi_{\mathrm{NL}} \cap \Phi_{\mathrm{A}}, g_j} \Bigg[\exp\Bigg(-s \sum_{\{j:\, x_j \in \Phi_{\mathrm{NL}} \cap \Phi_{\mathrm{A}},\, \|x_j\| > d_{\mathrm{eq}}^{-1}(R)\}} g_j K_{\mathrm{NL}} \|x_j\|^{-\beta_{\mathrm{NL}}} \Bigg) \Bigg].
\end{aligned} \tag{18}$$

By applying the Probability Generating Functional (PGFL) for SPPP[6] (which holds also in case of inhomogeneous SPPP [18]) to (18) and after some symbolic manipulation, we obtain the following result:

[6]Given an SPPP Φ and a function $f(x)$, the Probability Generating Functional allows us to compute the expectation of the product, i.e., $\mathbb{E}[\prod_{x \in \Phi}] = \exp(-\lambda \int_{\mathbb{R}^2} (1 - f(x)) \mathrm{d}x)$.

Result 3. *The Laplace transform $\mathcal{L}_{I_R}(s)$ for LOS/NLOS propagation with model given in* (1) *is:*

$$\mathcal{L}_{I_R}(s) = \exp\left(-2\pi\lambda_{\mathrm{I}} \int_{R}^{+\infty} \left[\frac{sK_{\mathrm{L}}v^{-\beta_{\mathrm{L}}}}{sK_{\mathrm{L}}v^{-\beta_{\mathrm{L}}}+\mu} \right] p_{\mathrm{L}}(v) v \mathrm{d}v \right)$$
$$\exp\left(-2\pi\lambda_{\mathrm{I}} \int_{d_{\mathrm{eq}}^{-1}(R)}^{+\infty} \left[\frac{sK_{\mathrm{NL}}v^{-\beta_{\mathrm{L}}}}{sK_{\mathrm{NL}}v^{-\beta_{\mathrm{NL}}}+\mu} \right] p_{\mathrm{NL}}(v) v \mathrm{d}v \right). \tag{19}$$

The Laplace transform in (19) along with (11) and (A.4) can be plugged in (5) to obtain the SINR CCDF through numerical integration.

G. Average Spectral Efficiency and Area Spectral Efficiency

First, we define the ASE over a given area A as the overall network throughput normalized over the area and the available bandwidth, i.e.,

$$\eta_{\mathrm{A}}(A) \triangleq \frac{T}{A \cdot \mathrm{BW_A}} = \frac{\mathrm{E[C]} \cdot \mathrm{BW_U} \cdot M}{A \cdot \mathrm{BW_A}}, \tag{20}$$

where T is the throughput of the network, $\mathrm{BW_A}$ is the available bandwidth, $\mathrm{BW_U}$ is the used bandwidth, $\mathrm{E[C]}$ is the average cell spectral efficiency,[7] M is the number of active BSs operating within A. The ASE of the network can be written as a function of the BS density and of the average spectral efficiency as follows:

$$\eta_{\mathrm{A}} \triangleq \lim_{A\to\infty} \eta_{\mathrm{A}}(A) \overset{(a)}{=} \lim_{A\to\infty} \frac{\mathrm{E[C]} \cdot \mathrm{BW_U} \cdot M}{A \cdot \mathrm{BW_A}} \overset{(b)}{=} \frac{\lambda_{\mathrm{A}} \cdot \mathrm{E[C]}}{N}, \tag{21}$$

where equality (a) is obtained by replacing $\lambda_{\mathrm{A}} = \lim_{A\to\infty} \frac{M}{A}$, while equality (b) follows from the definition of frequency reuse factor $N = \frac{\mathrm{BW_A}}{\mathrm{BW_U}}$. Similarly to [5, Section IV], the average rate $\mathrm{E[C]}$ can be computed as:

$$\mathrm{E[C]} = \mathrm{E}\left[\log_2(1+\gamma)\right] = \int_0^{+\infty} \mathbb{P}\left[\log_2(1+\gamma) > u\right] \mathrm{d}u$$
$$= \int_0^{+\infty} \int_0^{+\infty} \mathbb{P}\left[\log_2(1+\gamma) > u | r = R\right] f_r(R) \mathrm{d}R \mathrm{d}u$$
$$= \int_0^{+\infty} \int_0^{+\infty} e^{-\mu(2^u-1)K_{\mathrm{L}}^{-1}R^{\beta_{\mathrm{L}}}\sigma^2} \mathcal{L}_{I_R}\left(\mu(2^u-1)K_{\mathrm{L}}^{-1}R^{\beta_{\mathrm{L}}}\right) f_r(R) \mathrm{d}R \mathrm{d}u \tag{22}$$

where $\mathcal{L}_{I_R}(s)$ is given in (19). Similarly to the SINR CCDF, (22) can be evaluated numerically.

[7] In the system model we assume in this paper, the average cell spectral efficiency is the rate of a typical mobile user.

IV. Energy efficiency with LOS/NLOS propagation

A. Computing the transmit power per base station

We start by evaluating the BSs transmission power, in order to be able to compute the overall power consumption of the network. Ideally, the P_{TX} should be set in order to guarantee operation within the interference-limited regime,[8] i.e. the transmit power should be high enough so that the thermal noise power at the user receiver can be neglected with respect to the interference power at the receiver. In fact, when the network is in the interference-limited regime, the transmit power is high enough that any further increase of it would be pointless in terms of enhancing the SINR, since the receive power increment is balanced by the exact same interference increment.

In practice, the outage probability $\theta = \mathbb{P}\left[\gamma \leq \gamma_{\mathrm{th}}\right]$ is used to constraint the power necessary to operate within the interference limited regime. When the TX power is low, small increments of P_{TX} yields large improvements of the outage θ; however, as P_{TX} increases, the corresponding outage gain reduces, until θ eventually converges to its optimal value θ^*, which is reached in absence of thermal noise. It is reasonable to assume that the network is the interference-limited regime when the following condition is met:

$$|\theta^* - \theta| \leq \Delta_\theta, \tag{23}$$

where Δ_θ is a tolerance measure setting the constraint in terms of the maximum deviation of θ from the optimal value θ^*. Eq. (23) provides us with a metric to compute the transmit power, but does not give us any indication on how to find P_{TX} as a function of the density λ. Unfortunately, we cannot derive a closed-form expression for the transmit power that satisfies (23), as we do not have any closed-form solution for the outage probability $\theta = \mathbb{P}\left[\gamma \leq \gamma_{\mathrm{th}}\right]$. We then take a different approach to calculate the minimum transmit power.

In Alg. 1 we propose an iterative algorithm that finds the minimum transmit power satisfying (23) by using the numerical integration of (5). This algorithm computes the outage probability corresponding to a given P_{TX}; starting from a low value of power, it gradually increases P_{TX} by a power step Δ_P, until (23) is satisfied. To speed up this procedure, the step granularity is adjusted from a coarse step $\mathbb{P}_1$ up to the finest step $\mathbb{P}_{N_{\mathbf{P}}}$, which represents the precision of the power value returned by Alg. 1.

[8]This guarantees that the network performance is not limited by the transmitted power.

Algorithm 1 Steps to compute the transmit power.

INPUTS:

1) Vector of the power steps in dBm $\mathbf{p} = [\mathbb{P}_1, \cdots \mathbb{P}_{N_\mathbf{p}}]$, $\mathrm{N}_\mathbf{p}$ is the length of vector $\mathbf{p}$;
2) Outage SINR threshold γ_{th} and outage tolerance Δ_θ;

Initialize variables:

1) $P_{curr} = P_{N_0}$, where P_{N_0} is the AWGN power in dBm over the bandwidth $\mathrm{BW_U}$
2) $P_{\mathrm{fin}} = P_{curr}$

Find optimal outage $\theta^* = \mathbb{P}\left[\gamma \leq \gamma_{\mathrm{th}}\right]$ by integrating (5) with parameter $\sigma^2 = 0$

for $k = 1, \cdots, N_\mathbf{p}$ **do**

Find $\theta(P_{curr}) = \mathbb{P}\left[\gamma \leq \gamma_{\mathrm{th}}\right]$ by integrating (5) with parameter $\sigma^2 = 10^{-\frac{P_{curr}}{10}}$

Set granularity of the power step $\Delta_P = \mathbf{p}_k$

while $|\theta^* - \theta(P_{curr})| > \Delta_\theta$ **do**

Increase the current power with step Δ_P, i.e, $P_{curr} = P_{curr} + \Delta_P$

Find $\theta(P_{curr}) = \mathbb{P}\left[\gamma \leq \gamma_{\mathrm{th}}\right]$ by integrating (5) with parameter $\sigma^2 = 10^{-\frac{P_{curr}}{10}}$

Update the final value of power, i.e., $P_{\mathrm{fin}} = P_{curr}$

Remove the last power increment before increasing the granularity, i.e., $P_{curr} = P_{curr} - \Delta_P$

OUTPUT: P_{fin} is the power in dBm s.t. (23) is satisfied.

B. Energy efficiency

We now characterize the energy efficiency of the network as a function of the BS density λ to identify the trade-off between the ASE and the power consumed by network. We define the *energy efficiency* as the ratio between the overall throughput delivered by the network and the total power consumed by the wireless network, i.e., we define the energy efficiency as follows:

$$\eta_{\mathrm{EE}}(\lambda) \triangleq \frac{T(\lambda)}{P_{\mathrm{TOT}}(\lambda)}, \tag{24}$$

where $T(\lambda)$ is the network throughput, given as $T(\lambda) = A \cdot \mathrm{BW} \cdot \eta_{\mathrm{A}}(\lambda)$, with BW denoting the bandwidth and $\eta_{\mathrm{A}}(\lambda)$ denoting the ASE; P_{TOT} is the total power consumption of the network.

When we compute the power consumption of each BS, we need to take into account that a fraction of the BSs may be inactive and model the power consumption accordingly. For active BSs, we model the power consumption $P_{\mathrm{BS,A}}$ of the BS assuming that $P_{\mathrm{BS,A}}$ is the sum of two components, i.e., $P_{\mathrm{BS,A}} = P_0 + P_{\mathrm{RF}}$: (i) The first, denoted by P_0, takes into account the energy necessary for signal processing and to power up the base station circuitry. This power P_0 is modelled as a component being independent of the transmit power and of the BS load [21];

(ii) The second component, denoted by P_{RF}, takes into account the power fed into the power amplifier before the signal is transmitted. The power P_{RF} is assumed to be proportional to the power transmitted by the BS; we can thus write $P_{\mathrm{RF}} = K_{\mathrm{RF}} P_{\mathrm{TX}}$, where K_{RF} takes into account the losses of the power amplifier (i.e., we assume K_{RF} to be the inverse of the power amplifier efficiency). In the case of inactive base stations, we assume that the BS switches to a standby state for energy saving purposes [22], in which it does not transmit (i.e., $P_{\mathrm{RF}} = 0$) and reduces the circuitry power consumption. Therefore, the power required to maintain the standby state can be modelled as $P_{\mathrm{BS,S}} = \rho P_0$, where ρ is a power saving factor that reproduces the relative power consumption of the circuitry with respect to the active case; note that $0 < \rho < 1$. Finally, the total power consumption due to both active and inactive BS can be expressed as follows:

$$P_{\mathrm{TOT}} = A\lambda_{\mathrm{A}} P_{\mathrm{BS,A}} + A(\lambda - \lambda_{\mathrm{A}}) P_{\mathrm{BS,S}} = A\lambda_{\mathrm{A}} P_0 + A\lambda_{\mathrm{A}} P_{\mathrm{TX}} K_{\mathrm{RF}} + A(\lambda - \lambda_{\mathrm{A}})\rho P_0 \qquad (25)$$

The energy efficiency for the full and partial load regimes is addressed in the next sub-sections.

C. Energy efficiency in full load regime

We now study the energy efficiency $\eta_{\mathrm{EE}}(\lambda)$ trend as a function of λ; we focus on the full load regime, i.e., $p_{\mathrm{A}} = 1$ and $\lambda_{\mathrm{A}} = \lambda$. Unfortunately, the analysis of the derivative of η_{EE} is not straightforward, as we have a closed-form solution neither for the throughput $T(\lambda)$ nor for the transmit power $P_{\mathrm{TX}}(\lambda)$. One feasible way to get around this burden is to approximate $T(\lambda)$ and $P_{\mathrm{TX}}(\lambda)$ with functions in the form:

$$f(z) = az^b. \qquad (26)$$

The model in (26) has two advantages: (i) it can be differentiated and, thus, is apt to investigate the existence of optima; (ii) it is well suited to fit the non-linear behaviour of ASE and TX power. In fact, we have shown in our previous work [23] that both $T(\lambda)$ and $P_{\mathrm{TX}}(\lambda)$ can be approximated with a piece-wise function in the form (26); this approximation holds for both single-slope and LOS/NLOS model (1) for path-loss. Once the curves $T(\lambda)$ and $P_{\mathrm{TX}}(\lambda)$ have been computed using numerical integration, according to (21) and Algorithm 1, respectively, the parameters a and b can be obtained, for instance, by linear regression in the logarithmic domain for a given range of values of λ.

We approximate the throughput as $T(\lambda) = AT_0\lambda^{\alpha}$ and the transmit power as $P_{\mathrm{TX}}(\lambda) = P_{\mathrm{T}}\lambda^{\delta}$, within a given interval of λ [23]. Under these assumptions, the energy efficiency becomes:

$$\eta_{\mathrm{EE}}(\lambda) = \frac{T_0\lambda^{\alpha}}{\lambda P_0 + \lambda K_{\mathrm{RF}} P_{\mathrm{T}}\lambda^{\delta}} = \frac{T_0\lambda^{\alpha-1}}{P_0 + K_{\mathrm{RF}} P_{\mathrm{T}}\lambda^{\delta}}. \tag{27}$$

The derivative of $\eta_{\mathrm{EE}}(\lambda)$ is given below:

$$\frac{\mathrm{d}\eta_{EE}(\lambda)}{\mathrm{d}\lambda} = \frac{T_0P_0(\alpha-1)\lambda^{\alpha-2} + T_0K_{\mathrm{RF}}P_{\mathrm{T}}(\alpha-\delta-1)\lambda^{\alpha+\delta-2}}{\left(P_0 + K_{\mathrm{RF}}P_{\mathrm{T}}\lambda^{\delta}\right)^2}. \tag{28}$$

Let us note that T_0, P_0, K_{RF} and P_T are positive; moreover it is reasonable to assume that $\alpha > 0$ (i.e., the ASE is an increasing function of the density) and that $\delta < 0$, i.e., the transmit power per BS is a decreasing function of the density. In the following paragraphs, we study the behaviour of the energy efficiency as function of the density λ by analyzing the derivative $\eta'_{\mathrm{EE}}(\lambda)$. We distinguish the following three cases:

1) The energy efficiency is a monotonically increasing function: This occurs if the ASE growth is linear or superlinear, i.e., if $\alpha \geq 1$. It follows that $\alpha \geq 1 > 1 + \delta$ holds true; in this case, $\eta'_{\mathrm{EE}}(\lambda)$ is strictly positive, meaning that the energy efficiency increases with the density.

2) The energy efficiency is a monotonically decreasing function: This occurs if the ASE growth is sublinear, i.e., if $\alpha < 1$, and, in addition, $\alpha < 1 + \delta$. Then, $\eta'_{\mathrm{EE}}(\lambda)$ is strictly negative and so the energy efficiency is a monotonically decreasing function of the density λ.

3) The energy efficiency exhibits an optimum point: If ASE gain is sublinear (i.e. $\alpha < 1$) but grows with a slope α sufficiently high, (i.e., $\alpha > 1 + \delta$), then we obtain that the derivative $\eta\prime_{\mathrm{EE}}(\lambda)$ nulls for

$$\lambda_0 = \left(\frac{P_0\,(1-\alpha)}{K_{\mathrm{RF}}P_{\mathrm{T}}\,(\alpha-\delta-1)}\right)^{1/\delta}, \tag{29}$$

is positive for $\lambda < \lambda_0$ and is negative for $\lambda > \lambda_0$; and where λ_0 is a global maximum of $\eta_{\mathrm{EE}}(\lambda)$.

As a whole, the behavior of the spectral efficiency is due to how the growths of the ASE and the TX power relate among each other as λ increases. If the ASE grows rapidly enough to counterbalance the total power increase of the network given by the addition of new BSs, then the $\eta_{\mathrm{EE}}(\lambda)$ increases with the BS density; this means that adding extra BSs is profitable in terms of $\eta_{\mathrm{EE}}(\lambda)$; else, adding BSs turns not to be profitable from the $\eta_{\mathrm{EE}}(\lambda)$ point of view.

D. Energy efficiency in partial load regime

In this regime, we only analyze the case where $\lambda > \lambda_{\mathrm{U}}$, as the opposite case of $\lambda < \lambda_{\mathrm{U}}$ leads back to the full load regime. By using L'Hôpital's rule, one can show that (14) can be approximated by $p_{\mathrm{A}} \cong \lambda_{\mathrm{U}}\lambda^{-1}$, for λ sufficiently greater than λ_{U}. By applying this approximation to (25), we obtain:

$$P_{\mathrm{TOT}} = \lambda_{\mathrm{U}} P_0(1-\rho) + \lambda\rho P_0 + \lambda_{\mathrm{U}} K_{\mathrm{RF}} P_{\mathrm{T}} \lambda^{\delta}. \tag{30}$$

It is known from [21] that, as the BS density increases, the main contribution to the total power consumption is due to the circuitry power P_0, while the transmit power becomes negligible for the overall power balance. Therefore, to make the problem more tractable, we can further approximate the total power in (30) as $P_{\mathrm{TOT}} \cong \lambda_{\mathrm{U}} P_0(1-\rho) + \lambda\rho P_0$. From (24), by using the approximation $T(\lambda) = AT_0\lambda^{\alpha}$ for the throughput and $P_{\mathrm{TOT}} \cong \lambda_{\mathrm{U}} P_0(1-\rho) + \lambda\rho P_0$ for the power, we obtain the following expression for the energy efficiency:

$$\eta_{\mathrm{EE}}(\lambda) \cong \frac{T_0\lambda^{\alpha-1}}{\lambda_{\mathrm{U}} P_0(1-\rho) + \lambda\rho P_0}. \tag{31}$$

To analyze the behaviour of the energy efficiency as a function of λ, we follow the same approach as in Section IV-C and we compute the derivative of $\eta_{\mathrm{EE}}(\lambda)$, which is given below:

$$\frac{\mathrm{d}\eta_{EE}(\lambda)}{\mathrm{d}\lambda} = \frac{T_0\lambda^{\alpha-1}\left(\lambda\rho(\alpha-1) + \alpha\lambda_{\mathrm{U}}(1-\rho)\right)}{\left(\lambda_{\mathrm{U}} P_0(1-\rho) + \lambda\rho P_0\right)^2}. \tag{32}$$

As the ASE (and so the throughput) is known to be sub-linear in the partial load regime [4], [10], we assume $0 < \alpha < 1$; moreover, the power saving factor ρ satisfies $0 < \rho < 1$. Therefore, the derivative η'_{EE} nulls for:

$$\lambda^* = \frac{\alpha\lambda_{\mathrm{U}}(1-\rho)}{\rho(1-\alpha)}, \tag{33}$$

is positive for $\lambda < \lambda^*$ and negative for $\lambda > \lambda^*$. Hence, λ^* is a local maximum of the energy efficiency for the partial load regime and the energy efficiency decreases for densities $\lambda > \lambda^*$. Note that, this result holds for λ sufficiently greater than λ_{U}.

V. Results

In this section we present and discuss the results we obtained by integrating numerically the expressions of outage probability, of the Spectral Efficiency (SE), and of the ASE. In Section V-A, V-C and V-D we assume the network to be interference-limited, while the noise is taken into account in Section V-E and V-F. In regards to the validation of the analytical model presented

in Section III, we benchmarked it with simulation results. In particular, in the simulation we reproduced the same system model as described in Section II, with only a couple of differences with respect to the analytical one, namely:

(i) For LOS Case 1, the LOS probability function is modelled as (2) in the simulations, while we used (3) for the mathematical framework. For LOS Case 2, the same LOS probability function (i.e., (4)) is used for both analytical and simulated models;

(ii) the average number of BSs deployed within the network is infinite for the analytical model, while it is limited to 10^5 for the simulated one.

Let us note that we set the parameter L for the LOS probability function in (3) so as to make it reproduce as closely as possible the function (2) with the related values recommended by the 3GPP standard [15]; we adopted the same value of L for (4) as well. These details along with the remaining parameter settings we used to obtain the results are specified in Table II. Both numerical integrations and simulations have been carried out using Matlab; in regards to the simulations, the network performance have been obtained, first, by deploying a network of users and base stations with the specified probability distributions and, second, by evaluating the SINR and spectral efficiency — as $\log_2(1+\mathrm{SINR})$ — of the users. Since the whole mathematical framework is based on the evaluation of the SINR, we carried out the benchmark by computing the empirical SINR from the simulations and, then, by comparing the coverage probabilities (i.e., $\mathbb{P}\left[\mathrm{SINR} \leq \mathrm{Threshold}\right]$) obtained from the numerical integrations and the simulations, respectively.

A. Spectral efficiency, outage probability and ASE

In this subsection we assume the network to be in the full load regime and with frequency reuse 1. We compared the results for two LOS probability functions, namely (3) and (4); we also compared the results for LOS/NLOS propagation with those obtained with a the single slope path-loss model. We first analyze the outage probability (defined as $\theta = \mathbb{P}\left[\gamma \leq \gamma_{\mathrm{th}}\right]$) results, which have been obtained by numerical integration of (5).

We show the outage probability results in Fig. 3a, where we also compare the analytical results with those obtained through simulations. In this plot, we can see the impact of the LOS/NLOS propagation with respect to the single slope Path-Loss (PL). With single-slope PL, the outage is constant with the BS density. In contrast, with LOS/NLOS propagation, there is a minimum

TABLE II

PARAMETERS FOR RESULT SECTION

Parameter	**Value**
Path-loss - Single slope	$\mathrm{PL}_{\mathrm{SL}}(d_{\mathrm{km}}) = 140.7 + 36.7\log(d_{\mathrm{km}})$, $\beta = 3.67$, $K_{\mathrm{SL}} = 10^{-14.07}$ [15], for both analytical and simulated model
Path-loss - Combined LOS/NLOS	Eq. (1) with d in km, $K_{\mathrm{L}} = 10^{-10.38}$, $\beta_{\mathrm{L}} = 2.09$, $K_{\mathrm{NL}} = 10^{-14.54}$, $\beta_{\mathrm{NL}} = 3.75$ LOS function for LOS Case 1: Eq. (3) for the analytical model; Eq. (2) with $d_0 = 0.156\mathrm{km}$, $d_1 = 0.03\mathrm{km}$ [15] for the simulated model LOS function for LOS Case 2: Eq. (4) for both analytical and simulated models
Parameter L for eq. (3) and (4)	82.5m, set so that (2) and (3) intersect at the point corresponding to probability 0.5.
Bandwidth BW	10 MHz centered at 2 GHz
Noise	Additive White Gaussian Noise (AWGN) with -174 dBm/Hz Power Spectral Density
Noise Figure	9 dB
Antenna at BS and UE	Omni-directional with 0 dBi gain
SINR threshold	$\gamma_{\mathrm{th}} = -8$dB
Number of simulation snapshots	10^5
K_{RF}	10 [21]
P_0	10W [21]

in the outage curves, which is achieved for density λ = 50-100BSs/km^2, depending on the LOS probability function. Within this range of densities, the user is likely to be in LOS with the serving BS and in NLOS with most of the interfering BS, meaning that the interference power is lower than the received power.

At densities λ greater than 200BSs/km^2, the outage starts growing drastically and, depending on the LOS probability function, can reach 38-40%. This is due to an increase on the likelihood of the interfering BSs entering the LOS region, causing an overall interference growth and thus a reduction of the SIR. At densities λ smaller than 100BSs/km^2, the serving BS as well as the interfering BSs are likely to be in NLOS with the user. Because of this, both the receive power and the overall interference increase at the same pace[9] and, as a consequence, the SIR remains constant, and so does the outage. Let us note that, the LOS probability function affects the outage curves at intermediate values of the BS density (e.g. 10-300 BSs/km^2). At low densities,

[9]If both serving BS and interfering BS are in NLOS with the user, the path-loss exponents of the serving BS-to-user channel and of the interfering BS-to-user channels are the same and, therefore, the power or the interference and of the received signal varies with the same slope as a function of the density.

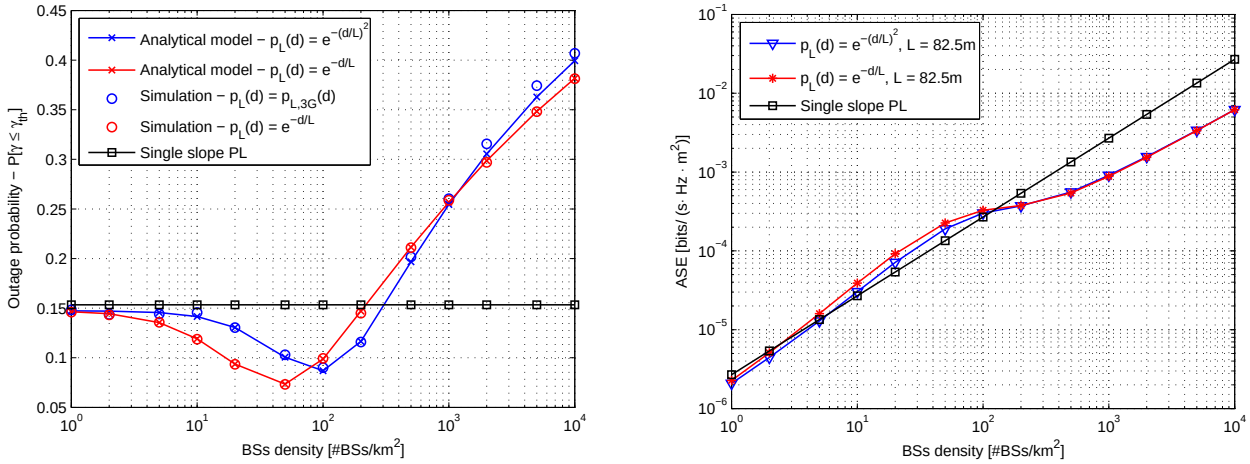

(a) Outage vs base station density.

(b) ASE vs base station density.

Fig. 3. (a) Outage probability and (b) ASE vs base station density for different LOS probability function. In (a), the analytical results are shown to match those obtained through simulations, with only a small deviation for blue curve, which is due to the approximation of the LOS probability function (2) with (3).

all the BSs are likely to be in NLOS with the user, while at high densities the serving BS and the strongest interferers are likely to be in LOS with the user.

The results of the ASE are shown in Fig. 3b. Compared to the single-slope PL, which shows a linear growth of the ASE with the density λ, with the LOS/NLOS propagation we observe a different behaviour of the ASE. In particular, we observe a lower steepness of the ASE curve at high BS densities, which is due to the effect of the interfering BSs entering the LOS region and, thus, increasing the total interference power.

To assess steepness of the ASE, we can use linear regression to interpolate the ASE curve with the model given in (26). In particular, we can approximate the ASE $\eta_{\mathrm{A}}(\lambda)$ with a piece-wise function of the kind $\eta_{\mathrm{A}}(\lambda) = \eta_{\mathrm{A},0}\lambda^{\alpha}$, where $\eta_{\mathrm{A},0}$ and α are given for given intervals of λ. We specifically focus on α, which gives the steepness of the ASE curve. With reference to the ASE curve (solid-blue curve in Fig. 3b) obtained with (3) as a LOS probability function, the value of the parameter α turns to be 1.15 within the range of λ 1-50 BSs/km^2, 0.48 within the range 50-500 BSs/km^2 and 0.81 within the range 500-10000 BSs/km^2.

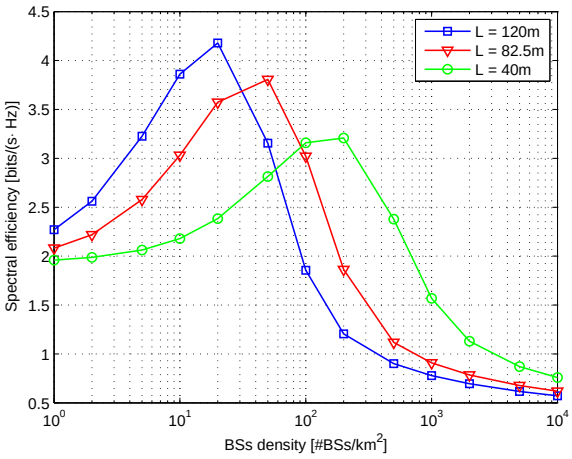

Fig. 4. Spectral efficiency vs base station density for fully loaded networks. These curves have been obtained using (3) as LOS probability function, for which we used three different values of the LOS likelihood parameter L.

B. *Effect of different LOS profiles*

In this paper we obtained the results by considering a given value L for the LOS probability function (see Table II) which, as explained at the beginning of Section V, is set in order to calibrate the analytical model with the system model provided by 3GPP for urban pico-cellular scenario. In this subsection, we investigate the effect that the parameter L has on the network performance; the related results are shown in Figure 4, where one can observe that the behaviour of the SE curve is influenced by the LOS probability. In fact, we notice that the density giving the highest spectral efficiency[10] depends on the LOS likelihood parameter L. To explain this, we should consider the optimal SE point, which occurs at the cell density where the user enters the LOS region around the serving BS but remains in NLOS with most of the interfering BSs. In denser propagation environments (e.g., L = 40m in Figure 4), the user will enter the LOS region of the serving BS in at higher cell densities, compared to the case of dense propagation environments; hence, the optimal value of the spectral efficiency will be reached at a higher BS density, and vice-versa.

[10]The reason why the spectral efficiency is not constant but has a maximum value with the cell density is the same as for the minimum coverage we can observe in Figure 3a; the reader can refer to the explanation we gave above.

C. Frequency reuse

To have a comprehensive view of the frequency reuse as an interference mitigation scheme, we need to assess the trade-off between the ASE and the network coverage probability, defined as $1-\mathbb{P}\left[\gamma \leq \gamma_{\text{th}}\right]$. The results of this trade-off are shown in Fig. 5, where we plotted the network coverage against the ASE for different frequency reuse factors and base station densities.

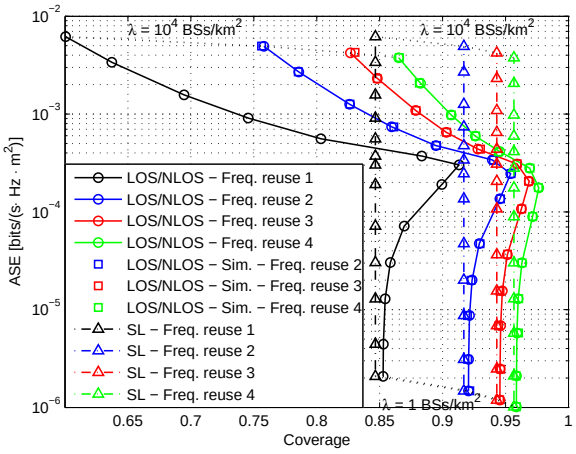

Fig. 5. ASE vs coverage trade-off for frequency reuse. The trade-off curves have been plotted for BS density equal to 1, 2, 5, 10, 20, 50, 100, 200, 500, 1000, 2000, 5000, 10000 BSs/km^2, and compare the combined LOS/NLOS model with the single slope one.

Firstly, we focus on the LOS/NLOS propagation; we can notice from this plot that, if we fix the BS density, higher frequency reuse factors enhance the network coverage but, on the other hand, determine a drop of the ASE. This is in line with what one would expect from frequency reuse. Nonetheless, if we have no constraint in the choice of the BS density, the ASE vs coverage trade-off improves as the frequency reuse factor N increases. In fact, the trade-off curve we obtain for a given reuse factor N lies on the top-right hand side with respect to the curve for reuse factor $N-1$. This means that, by increasing the reuse factor and the base station density at the same time, it is possible to achieve better performance than with a lower frequency reuse factors; note, though, that this is true when there is no constraint in terms of BS density. This is actually a surprising results, as one might think that increasing the frequency reuse factor leads to a drastic drop of the area spectral efficiency, due to the usage of only one N-th of the available bandwidth. However, it turns out that the interference reduction obtained by limiting each cell spectrum usage counterbalances the spectral efficiency decrease due to this spectrum

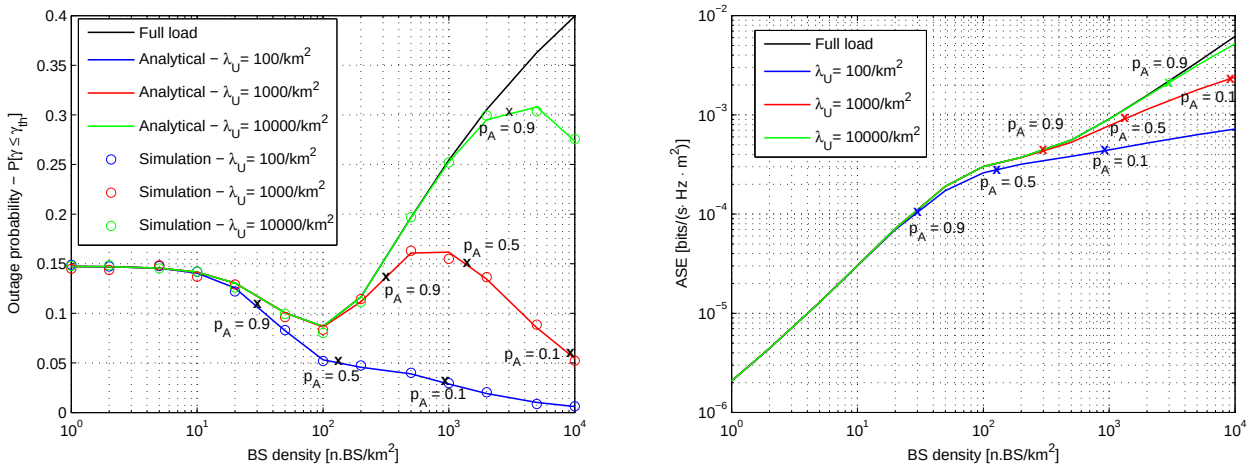

(a) Outage vs base station density

(b) Spectral efficiency vs base station density.

Fig. 6. The probability p_{A} given by (14) is reported as an "x" on each curve. The outage probability has been obtained for $\gamma_{\mathrm{th}} = -8$dB. In (a), the analytical results are shown to match closely those obtained through simulations.

limitation and, thus, provides an overall gain in the ASE vs. coverage trade-off, as the density increases. From the plot in Fig. 5 we can conclude that frequency ALOHA turns to be a simple but effective resource management technique for dense networks, which would otherwise face serious coverage issues due to the effect of LOS/NLOS propagation.

By looking at the single slope PL curve in Fig. 5, it appears that higher frequency reuse factors should still be preferred in order to improve the ASE vs coverage trade-off. However, unlike with the LOS/NLOS path loss, increasing the BS density enhances the ASE with no loss in terms of network coverage. Yet, modelling the signal propagation with the combined LOS/NLOS path loss yields different results than with the single-slope PL.

D. Partial load regime

In this subsection we show the results for the partial load regime with LOS/NLOS propagation. Differently from the case of full load regime, we recall that a fraction of the BSs may be inactive and, thus, the density of interfering BSs λ_{I} does not necessary follow the trend of BS density λ (see Section III-E and Fig. 2). In Fig. 6a and 6b we show the outage probability and the ASE curves, respectively, as functions of the BS density for difference user densities. To better understand the effect of the partial load on the network performance, we compare these curves with those of the full load regime. Furthermore, we higlight the values of the probability p_{A} of a BS being active over the outage and ASE curves.

We observe that, as long as $p_{\mathrm{A}} \geq 0.9$, the deviation from the full load regime is minimal. However, as soon as λ approaches the value of user density λ_{U}, the probability p_{A} drops and, as a consequence, the density of interfering λ_{I} BSs grows slowly with λ, up to the point where it saturates and converges to λ_{U} (see Fig. 2). At the same time, as λ increases, the distance from UE to the serving BS tends to decrease, leading to an increment of the received power. Overall, the fact that λ_{I} saturates whereas the received power keeps growing as λ increases has a positive impact on the SIR; as a result, the outage probability (see Fig. 6a) and the spectral efficiency improve once the density λ approaches or overcomes λ_{U}. Based on the results we show in Fig. 6a, we can notice that the partial load regime almost completely compensates the huge outage growth occurring at high densities due to LOS/NLOS propagation. Although this would be achieved at the cost of a massive BS deployment, steering the networks into the partial load regime represents an effective strategy to combat the network coverage issues resulting as a consequence of the LOS/NLOS propagation.

In regards to the ASE trend, we show the results in Fig. 6b. According to (21), the ASE trend is the combined outcome of the increase of the spectral efficiency and of the density of the active base stations. As the density of base stations increases and approaches the user density λ_{U}, the density of active base stations will converge to λ_{U} (see Fig. 6a); given that the density of active BSs remains constant, the only contribution to the ASE increase will be given by the spectral efficiency improvement. As a matter of fact, we can see that, with respect to full load regime, the ASE curves show a lower gain when the density λ approaches λ_{U}.

To assess steepness of the ASE, we applied linear regression to the ASE curves in order to obtain the value of the parameter α corresponding to different intervals of λ; we specifically consider the approximation for the curve corresponding to $\lambda_{\mathrm{U}} = 1000$UEs/km^2 (red curve in Fig. 6b). These values are $\alpha = 1.15$ within the density range 1-50 BSs/km^2, $\alpha = 0.43$ within the density range 50-500 BSs/km^2 and $\alpha = 0.46$ within the density range 500-10000 BSs/km^2.

E. Transmit power per base station

In Fig. 7 we show the simulation results of the transmit power per base station $P_{\mathrm{TX}}(\lambda)$, which has been computed by using Algorithm 1 exposed in Section IV-A. In this figure we compare the results we obtained using the *single slope* and the *combined LOS/NLOS* path loss models.

As we can see from this plot, the behaviour of the transmit power as a function of the BS

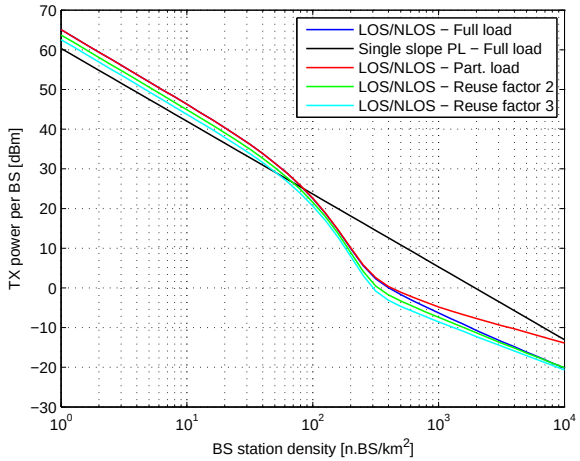

Fig. 7. Transmit power per BS. The power has been obtained with an SINR threshold $\gamma_{\mathrm{th}} = -8$dB and for tolerance $\Delta_\theta = 0.1\%$. The plot compares the TX power per BS for single slope-slope and LOS/NLOS path-loss for fully loaded networks. It also provides the curve for frequency reuse factor 2 and 3 and for partially loaded network with $\lambda_{\mathrm{U}} = 1000$UEs/km^2.

density λ is different in the two cases of single slope and combined LOS/NLOS propagation. With reference to Fig. 7, with single slope path loss, the power decreases linearly (in logarithmic scale) with the density; in the case of combined LOS/NLOS propagation, the transmit power exhibits different slopes as the base station density increases. We used linear regression to assess the slopes of the TX power curves (indicated by δ, as explained in Section IV-C) within different density intervals. With reference to the curve corresponding to fully loaded networks with LOS/NLOS propagation (solid-blue curve in Fig. 7), the values of (P_{T}, δ) are $(9.3 \cdot 10^{-9}, -1.9)$ within the λ range 1-60 BSs/km^2, $(4.4 \cdot 10^{-17}, -3.9)$ within the λ range 60-300 BSs/km^2 and $(1.15 \cdot 10^{-9}, -1.44)$ within the range 300-10000BSs/km^2.

The fact that the transmit power per base station decays more or less steeply with the density λ depends on how quickly the interference power increases or decreases with λ. As we explained in Section IV-A, the transmit power per base station $P_{\mathrm{TX}}(\lambda)$ has to be set so that the network is interference limited. Thus, if the channel attenuation between the interferer and the user decreases quickly as the density increases, a lower transmit power will be enough to guarantee that the interference power is greater than the noise power. In other words, if the interferer-to-user channel attenuation tends to decrease quickly as the density increases, so does the transmit power and vice-versa. For instance, for $\lambda \in [60, 300]$BSs/km^2, the probability of having interferers in LOS with the user rises and, as a consequence, we have a lower attenuation of the channel between

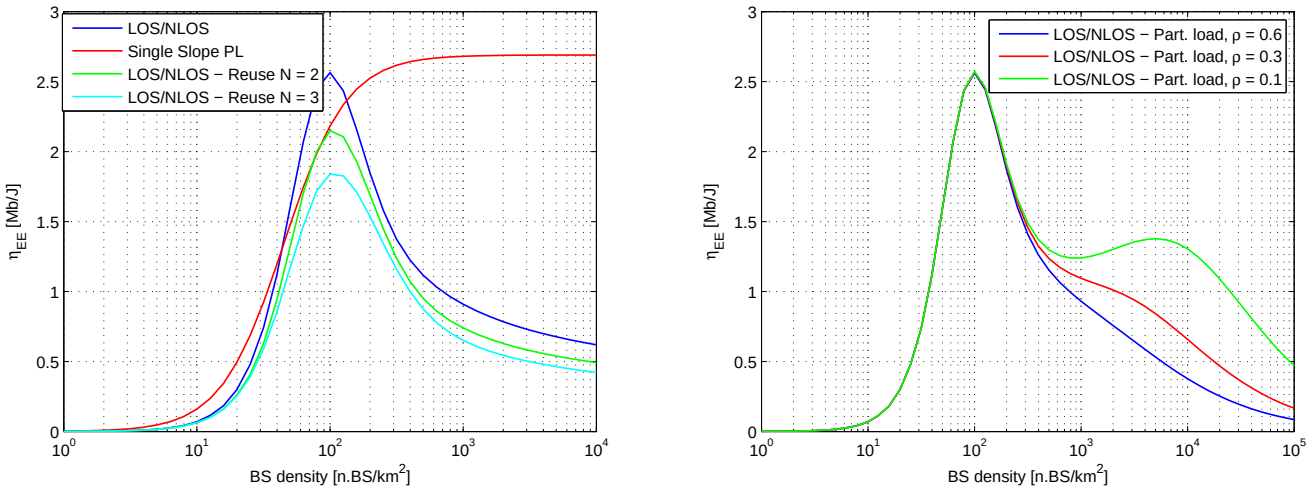

(a) Energy efficiency for fully loaded networks.

(b) Energy efficiency for partially loaded networks.

Fig. 8. (a) Energy efficiency vs BS density in full load regime. The plot compares the energy efficiency for LOS/NLOS with single slope path-loss. The energy efficiency is given also for frequency reuse factors 2 and 3. (b) Energy efficiency vs BS density for partially loaded networks. Curves are given for $\lambda_{\mathrm{U}} = 1000$UEs/km^2 and for three values of ρ.

the interfering base station and the user. Hence, the $P_{\mathrm{TX}}(\lambda)$ which guarantees the interference-limited regime will also decrease steeply with $\delta = -3.9$ as λ increases. On the contrary, for $\lambda > 300$ BSs/km^2, most of the interferers will have already entered the LOS zone, meaning that the interferer-to-user channel attenuation drops less rapidly than for $\lambda < 300$ BSs/km^2; for this reason, also $P_{\mathrm{TX}}(\lambda)$ will decrease less rapidly with $\delta = -1.44$.

Let us note that, with increasing reuse factors N, the TX power decreases, as indeed a smaller bandwidth is used and, thus, the noise power is lower.

F. Energy efficiency

One of the most surprising outcomes of our study on LOS/NLOS propagation for ultra-dense networks is the effect of cell-densification on the energy efficiency within the full load regime, of which we show the results in Fig. 8a. The difference between the energy efficiency with single-slope and with LOS/NLOS path-loss is noticeable. In the case of single-slope PL, due to the linear growth of the ASE, $\eta_{\mathrm{EE}}(\lambda)$ is a monotonically increasing function of the density λ (see Section IV-C1). In the case of LOS/NLOS propagation, from Fig. 8a we observe that the energy efficiency exhibits a maximum, which is achieved for a given density λ_0.

To explain this, we consider the case of frequency reuse $N = 1$ (solid-blue curve in Fig. 8a);

from (29) and with the values of the parameters P_0 (given in Table II), P_{T} and δ (given in Section V-E), and α (given in Section V-A), the optimal point λ_0 is approximately 100BSs/km^2. Beyond this point, the ASE gain is too low to compensate power consumption increase in the network, leading to a drop in terms of energy efficiency. From Fig. 8a, we can note that frequency reuse reduces the energy efficiency compared to $N = 1$. As a result of the lower ASE achieved at higher frequency reuse factors N, the energy efficiency drops as N increases.

In Fig. 8b we show the energy efficiency for the partial load regime, for a user density λ_{U} of 1000 UEs/km^2. As we are dealing with networks in the partial load regime, we are interested in the BS densities $\lambda > \lambda_{\mathrm{U}}$, where energy efficiency strongly depends on the power saving factor ρ of the BSs in stand-by state. This is because the parameter ρ determines the energy saving of the inactive BSs, which become more numerous as the density λ increases. Depending on the value of ρ, according to (33) a local maximum may even occur at $\lambda^* = \frac{\alpha\lambda_{\mathrm{U}}(1-\rho)}{\rho(1-\alpha)}$.

With $\rho = 0.1$ and with the values of α given in Section V-D, the local maximum turns to be $\lambda^* \cong 7300$BSs/km^2. For higher values of ρ, λ^* is smaller than or too close to λ_{U} to be considered as a reliable estimate of a maximum; we recall from Section IV-D that this estimate can be reckoned as reliable only if λ^* is sufficiently greater than λ_{U}. In fact, we observe from Fig. 8b that there is no local maximum beyond λ_{U} for $\rho = 0.3$ or 0.6. Based on our system model for ultra-dense networks which includes both LOS/NLOS propagation and partial load regime, from the results in Fig. 8b, we show the existence of two optimal operating points which turn to be convenient in terms of energy efficiency for the network operator. The first one can be achieved in full load regime, provided that the operator deploys the network with BS density given by (29); the second, by (33), occurs in the partial load regime and can be achieved only if the power saving factor is low enough (e.g., $\rho \approx 0.1$).

VI. Conclusions

In this paper, we have proposed a stochastic geometry-based framework to model the outage probability and the Area Spectral Efficiency (ASE) of Ultra-Dense Networks (UDNs), which can operate either in the full or partial load regimes, and where the signal propagation accounts for LOS and NLOS components.

As the main findings of our work, we have shown that, with LOS/NLOS propagation, massive cell densification determines a deterioration of the network coverage at high cell densities, if

the network is fully loaded. Moreover, the ASE grows less steeply than a linear function at high cell densities, which implies that a larger number of base stations would be required to achieve a given throughput target with respect to the case of single slope path-loss. However, from our results it also emerges that the coverage issues due to LOS/NLOS propagation can be mitigated by steering the network into the partial load regime; in addition, provided there is no constraint in terms of BS density, we showed that frequency ALOHA with frequency reuse factor N enhances the ASE vs. coverage trade-off with respect to a full frequency reuse case; moreover, this improvement further increases with the frequency reuse factor N.

We have extended our study also to the energy efficiency as a function of the BS density. We have shown that, as a combined effect of the LOS/NLOS propagation and of the partial load regime, there are two optimal points of the energy efficiency, one of which occurs in the full load regime, while the second is achieved at higher densities, when the network is in the partial load regime. Our work gives an insight in terms of the optimal density as a design parameter to optimize the energy efficiency of ultra-dense networks.

APPENDIX A
PDF OF THE DISTANCE TO THE SERVING BS

Once the LOS probability function is known, from (11) we obtain the PDF of the distance to the closest BS as follows:

$$\mathbb{P}\left[r > R\right] = \exp\left(-\lambda \int_{B(0,R)} p_{\mathrm{L}}(\|x\|)\mathrm{d}x \right) \exp\left(-\lambda \int_{B\left(0,d_{\mathrm{eq}}^{-1}(R)\right)} \left(1 - p_{\mathrm{L}}(\|x\|)\right) \mathrm{d}x \right). \quad \text{(A.1)}$$

Assuming the integrals in (A.1) can be solved in a closed-form, with some symbolic manipulation, (A.1) solves in its general form as follows:

$$\mathbb{P}\left[r > R\right] = \prod_{m=1}^{M} \exp(f_m(R)). \quad \text{(A.2)}$$

By taking the derivative of (A.2), we obtain:

$$\frac{\mathrm{d}}{\mathrm{d}R}\left[\mathbb{P}\left[r > R\right]\right] = \frac{\mathrm{d}}{\mathrm{d}R}\left[\prod_{m=1}^{M} \exp(f_m(R))\right] = \sum_{m=1}^{M} \frac{\mathrm{d}}{\mathrm{d}R}\left[\exp(f_m(R))\right] \prod_{n=1, n\neq m}^{M} \exp(f_n(R)) =$$

$$\sum_{m=1}^{M} \frac{\mathrm{d}}{\mathrm{d}R}\left[f_m(R)\right] \exp(f_m(R)) \prod_{n=1, n\neq m}^{M} \exp(f_n(R)) = \sum_{m=1}^{M} f'_m(R) \prod_{n=1}^{M} \exp(f_n(R)) =$$

$$\sum_{m=1}^{M} f'_m(R) \left(\prod_{n=1}^{M} \exp(f_n(R)) \right) = \mathbb{P}\left[r > R\right] \sum_{m=1}^{M} f'_m(R). \tag{A.3}$$

The PDF of the distance to the serving BS can finally be obtained as

$$f_r(R) = -\frac{\mathrm{d}}{\mathrm{d}R}\left[\mathbb{P}\left[r > R\right]\right] = -\mathbb{P}\left[r > R\right] \sum_{m=1}^{M} f'_m(R). \tag{A.4}$$

If we assume the LOS probability to be given by (3), we can further develop (A.1) by solving the integrals in (A.1) and, with further symbolic manipulation, we obtain:

$$\mathbb{P}\left[r > R\right] = e^{\pi\lambda L^2 e^{-\frac{R^2}{L^2}}} \cdot e^{-\pi\lambda L^2 e^{-\frac{R_{\mathrm{eq}}^2}{L^2}}} \cdot e^{-\pi\lambda R_{\mathrm{eq}}^2}, \tag{A.5}$$

where $R_{\mathrm{eq}} = d_{\mathrm{eq}}^{-1}(R)$. Let us define the functions $f_1(R)$, $f_2(R)$, $f_3(R)$ and their first derivatives $f'_1(R)$, $f'_2(R)$, and $f'_3(R)$, respectively, as follows:

$$f_1(R) = \pi\lambda L^2 e^{-\frac{R^2}{L^2}}, \quad f_2(R) = -\pi\lambda L^2 e^{-\frac{R_{\mathrm{eq}}^2}{L^2}}, \quad f_3(R) = -\pi\lambda R_{\mathrm{eq}}^2, \quad f'_1(R) = -2\pi\lambda R e^{-\frac{R^2}{L^2}},$$

$$f'_2(R) = \pi\lambda K_{\mathrm{eq}}^2 2\beta_{\mathrm{eq}} R^{2\beta_{\mathrm{eq}}-1} e^{-\frac{-K_{\mathrm{eq}}^2 R^{2\beta_{\mathrm{eq}}}}{L^2}}, \qquad f'_3(R) = -\pi\lambda K_{\mathrm{eq}}^2 2\beta_{\mathrm{eq}} R^{2\beta_{\mathrm{eq}}-1}.$$

By plugging (A.5) and $f'_1(R)$, $f'_2(R)$, and $f'_3(R)$ in (A.4), we obtain the PDF of the distance to the serving BS.

When the LOS probability function is given by (4), we obtain the PDF of distance to the closest BS station as follows. First, by solving the integrals in (A.1) and by some additional algebraic operations, we obtain $\mathbb{P}\left[r > R\right]$ as follows:

$$\mathbb{P}\left[r > R\right] = e^{2\pi\lambda L^2 e^{-\frac{R}{L}}} \cdot e^{2\pi\lambda L R e^{-\frac{R}{L}}} \cdot e^{-\pi\lambda R_{\mathrm{eq}}^2} \cdot e^{-2\pi\lambda L^2 e^{-\frac{R_{\mathrm{eq}}}{L}}} \cdot e^{-2\pi\lambda L R_{\mathrm{eq}} e^{-\frac{R_{\mathrm{eq}}}{L}}}. \tag{A.6}$$

Then, we define the functions $f_1(R)$, $f_2(R) \cdots$, $f_5(R)$ and we compute their respective derivatives $f'_1(R)$, $f'_2(R) \cdots$, $f'_5(R)$ as follows:

$$f_1(R) = 2\pi\lambda L^2 e^{-\frac{R}{L}}, \quad f'_1(R) = -2\pi\lambda L e^{-\frac{R}{L}}, \quad f_2(R) = 2\pi\lambda L R e^{-\frac{R}{L}}, \quad f'_2(R) = -2\pi\lambda (L-R) e^{-\frac{R}{L}},$$

$$f_3(R) = -\pi\lambda R_{\mathrm{eq}}^2, \quad f'_3(R) = -\pi\lambda K_{\mathrm{eq}}^2 2\beta_{\mathrm{eq}} R^{2\beta_{\mathrm{eq}}-1}, \quad f_4(R) = -2\pi\lambda L^2 e^{-\frac{R_{\mathrm{eq}}}{L}},$$

$$f'_4(R) = 2\pi\lambda L K_{\mathrm{eq}} \beta_{\mathrm{eq}} R^{\beta_{\mathrm{eq}}} e^{-\frac{K_{eq} R^{\beta_{\mathrm{eq}}}}{L}}, \quad f_5(R) = -2\pi\lambda L R_{\mathrm{eq}} e^{-\frac{R_{\mathrm{eq}}}{L}},$$

$$f'_5(R) = 2\pi\lambda L K_{\mathrm{eq}} \beta_{\mathrm{eq}} R^{\beta_{\mathrm{eq}}-1} (K_{\mathrm{eq}} R^{\beta_{\mathrm{eq}}} - L) e^{-\frac{K_{eq} R^{\beta_{\mathrm{eq}}}}{L}},$$

Finally, the PDF can be obtained by plugging $f'_1(R)$, $f'_2(R) \cdots$, $f'_5(R)$ and (A.6) in (A.4).

APPENDIX B
BENCHMARK OF PROBABILITY p_{A}

In this paper we assume that the user associates to the base station from which the path-loss is the minimum. When the path-loss is modelled as a single slope function, user association based on minimum path-loss is equivalent to user association based on the minimum distance from the base station [5], [13]. Using an empirical expression for the PDF of the Voronoi's cell area (which can be found in [24]), the authors of [13] computed an approximation of the probability of a Voronoi cell being empty, which corresponds to the complementary event of a base station being active defined in Section II-C.

Nevertheless, when the path-loss has both LOS and NLOS components, the user association is no longer equivalent to the minimum distance association rule. Moreover, it makes no longer sense to talk about Voronoi's cells, as the path-loss in (1) is a stochastic process, meaning the it is not possible to define the boundary of the cells in a deterministic way. It follows that (14) needs to be further validated in order to extend its use to the LOS/NLOS propagation case.

Motivated by our simulation results, we have noticed though that the effect of the propagation model given in (1) and (2) has a marginal effect on the on the probability p_{A} with respect to what given by (14) for the minimum distance user association. In Fig 9, we compared the simulation results of the probability p_{A} in the case of LOS/NLOS with (14) for various values of the base station density λ; as we can see from this plot, the maximum deviation from (14) is less than 2%, meaning that the model in (14) can be considered a reliable approximation of p_A also in case of LOS/NLOS propagation.

REFERENCES

[1] I. Hwang, B. Song, and S. S. Soliman, "A holistic view on hyper-dense heterogeneous and small cell networks," *IEEE Communications Magazine*, vol. 51, no. 6, pp. 20–27, Jun. 2013.

[2] N. Bhushan, L. Junyi, D. Malladi, R. Gilmore, D. Brenner, A. Damnjanovic, R. Sukhavasi, and S. Geirhofer, "Network Densification: the Dominant Theme for Wireless Evolution into 5G," *IEEE Communications Magazine*, 2014.

[3] Ericsson, "Ericsson White paper: 5G radio access," Feb. 2015. [Online]. Available: www.ericsson.com/res/docs/whitepapers/wp-5g.pdf

[4] J. Park, S.-L. Kim, and J. Zander, "Asymptotic behavior of ultra-dense cellular networks and its economic impact," in *IEEE Global Communications Conference (GLOBECOM 2014)*, Dec. 2014, pp. 4941–4946.

[5] J. G. Andrews, F. Baccelli, and R. K. Ganti, "A Tractable Approach to Coverage and Rate in Cellular Networks," *IEEE Trans. Wireless Commun.*, vol. 59, no. 11, pp. 3122–3134, 2011.

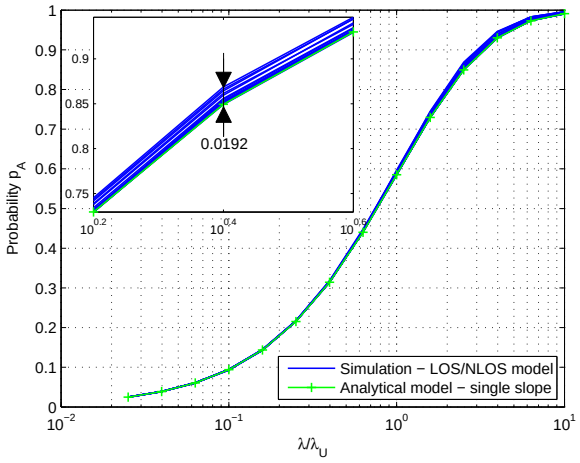

Fig. 9. Benchmark of probability p_{A}. The plot compares (14) (i.e., green curve) with the p_A curves (i.e., blue curves) obtained through simulation, for the propagation model in (1) and (2) and for various values of lambda. The relative difference (in terms of magnitude) with respect to the analytical model is less than 2%.

[6] X. Zhang and J. G. Andrews, "Downlink Cellular Network Analysis with Multi-slope Path Loss Models," 2014. [Online]. Available: http://arxiv.org/abs/1408.0549

[7] T. Bai, R. Vaze, and R. W. Heath, "Analysis of Blockage Effects on Urban Cellular Networks," *IEEE Trans. Wireless Commun.*, vol. 13, no. 9, pp. 5070–5083, Sep. 2014.

[8] C. Galiotto, N. K. Pratas, N. Marchetti, and L. Doyle, "A Stochastic Geometry Framework for LOS/NLOS Propagation in Dense Small Cell Networks," *IEEE ICC 2015*, 2015. [Online]. Available: http://arxiv.org/abs/1412.5065v2

[9] M. Ding, P. Wang, D. Lopez-Perez, G. Mao, and Z. Lin, "Performance Impact of LoS and NLoS Transmissions in Small Cell Networks," Mar. 2015. [Online]. Available: http://arxiv.org/abs/1503.04251

[10] C. Li, J. Zhang, and K. B. Letaief, "Throughput and Energy Efficiency Analysis of Small Cell Networks with Multi-Antenna Base Stations," *IEEE Transactions on Wireless Communications*, vol. 13, no. 5, pp. 2505 – 2517, Mar. 2014.

[11] T. Bai and R. W. Heath, "Coverage and Rate Analysis for Millimeter-Wave Cellular Networks," *IEEE Trans. Wireless Commun.*, vol. 14, no. 2, pp. 1536–1276, Oct. 2014.

[12] J. G. Andrews, "Seven Ways that HetNets Are a Cellular Paradigm Shift," *IEEE Communications Magazine*, vol. 51, no. 3, pp. 136 – 144, Mar. 2013.

[13] S. Lee and K. Huang, "Coverage and Economy of Cellular Networks with Many Base Stations," *IEEE Commun. Lett.*, vol. 16, no. 7, pp. 1038–1040, Jul 2012.

[14] H. S. Dhillon, R. K. Ganti, and J. G. Andrews, "Load-Aware Modeling and Analysis of Heterogeneous Cellular Networks," *IEEE Transactions on Wireless Communications*, vol. 12, no. 4, pp. 1666–1677, Apr. 2013.

[15] 3rd Generation Partnership Project (3GPP), "Further Advancements for E-UTRA Physical Layer Aspects (Release 9)," Mar. 2010, 3GPP TR 36.814 V9.0.0 (2010-03).

[16] J. Park, S.-L. Kim, and J. Zander, "Tractable Resource Management With Uplink Decoupled Millimeter-Wave Overlay in Ultra-Dense Cellular Networks," *IEEE Transactions on Wireless Communications*, vol. 15, no. 6, pp. 4362 – 4379, 2016.

[17] B. Błaszczyszyn, M. K. Karrayy, and P. Keelerz, “Wireless networks appear Poissonian due to strong shadowing,” *IEEE Transactions on Wireless Communications*, vol. PP, no. 99, pp. 1–1, 2015.

[18] M. Haenggi, *Stochastic Geometry for Wireless Networks*. Cambridge Press, 2013.

[19] F. Baccelli and B. Błaszczyszyn, *Stochastic Geometry and Wireless Networks, Volume I, Theory*. NOW Publishers, 2009.

[20] V. Chandrasekhar and J. G. Andrews, “Spectrum Allocation in Tiered Cellular Networks,” *IEEE Transaction on Communications*, vol. 57, no. 10, pp. 3059 – 3068, October 2009.

[21] G. Auer, V. Giannini, C. Desset, I. Gódor, P. Skillermark, M. Olsson, M. A. Imran, D. Sabella, M. J. Gonzalez, O. Blume, and A. Fehske, “How Much Energy Is Needed to Run a Wireless Network?” *IEEE Wireless Commun.*, vol. 18, pp. 40 – 49, Oct. 2011.

[22] I. Ashraf, F. Boccardi, and L. Ho, “SLEEP mode techniques for small cell deployments,” *IEEE Communications Magazine*, vol. 49, no. 8, pp. 72–79, Aug. 2011.

[23] C. Galiotto, I. M. Gomez, N. Marchetti, and L. Doyle, “Effect of LOS/NLOS Propagation on Area Spectral Efficiency and Energy Efficiency of Small-Cells,” *IEEE Globecom 2014*, 2014. [Online]. Available: http://arxiv.org/abs/1409.7575

[24] J.-S. Ferenc and Z. Néda, “On the size distribution of Poisson Voronoi cells,” *Physica A: Stat. Mechanics and its App.*, vol. 385, no. 2, p. 518âĂŞ526, 2007. [Online]. Available: http://arxiv.org/abs/cond-mat/0406116